fractal and fractional

MDPI

Article

Fractional View Analysis System of Korteweg–de Vries Equations Using an Analytical Method

Yousef Jawarneh, Zainab Alsheekhhussain and M. Mossa Al-Sawalha *

Department of Mathematics, College of Science, University of Ha'il, Ha'il 2440, Saudi Arabia; y.jawaneh@uoh.edu.sa (Y.J.); za.hussain@uoh.edu.sa (Z.A.)
* Correspondence: m.alswalha@uoh.edu.sa

Abstract: This study introduces two innovative methods, the new transform iteration method and the residual power series transform method, to solve fractional nonlinear system Korteweg–de Vries (KdV) equations. These equations, fundamental in describing nonlinear wave phenomena, present complexities due to the involvement of fractional derivatives. In demonstrating the application of the new transform iteration method and the residual power series transform method, computational analyses showcase their efficiency and accuracy in computing solutions for fractional nonlinear system KdV equations. Tables and figures accompanying this research present the obtained solutions, highlighting the superior performance of the new transform iteration method and the residual power series transform method compared to existing methods. The results underscore the efficacy of these novel methods in handling complex nonlinear equations involving fractional derivatives, suggesting their potential for broader applicability in similar mathematical problems.

Keywords: analytical solutions; new transform iteration method; caputo operator; fractional Korteweg–de Vries equations; residual power series transform method; nonlinear system of partial differential equations

Citation: Jawarneh, Y.; Alsheekhhussain, Z.; Al-Sawalha, M.M. Fractional View Analysis System of Korteweg–de Vries Equations Using an Analytical Method. *Fractal Fract.* **2024**, *8*, 40. https://doi.org/10.3390/fractalfract8010040

Academic Editors: Haci Mehmet Baskonus and Yusuf Gürefe

Received: 7 December 2023
Revised: 1 January 2024
Accepted: 4 January 2024
Published: 7 January 2024

1. Introduction

The vast applicability of fractional calculus has become an essential resource in today's world. Due to its relevance to several branches of applied science and engineering, this field has attracted the attention of mathematicians and other experts for more than 300 years. Classical differential equations of integer order may be extended to the fractional order using fractional calculus. One major benefit of using fractional differential equations is their non-local nature. This allows for the development of a wide variety of mathematical models, as the next stage of a system depends on both its current state and all of its previous states [1–10].

Fractional coupled systems are often used to study plasma's multi-component behaviour, including ions, free electrons, and atoms. A lot of researchers have endeavoured to evaluate this behaviour. Paul Kersten and Joseph Krasil'shchik have recently studied the Korteweg–de Vries (KdV) and modified KdV (mKdV) equations. They have proposed a nonlinear system analysis method based on the absolute complexity between a couple of KdV–mKdV systems [11–14]. Various versions of this Kersten–Krasil'shchik linked KdV–mKdV nonlinear system have been suggested by various researchers [15–19]. A mathematical model for the behaviour of multi-component plasma for waves moving down the positive zeta axis is provided by the nonlinear fractional Kersten–Krasil'shchik coupled KdV–mKdV system, and one of these variants is as follows:

$$
\begin{aligned}
&D_{\lambda}^{p} v_1(\alpha,\lambda) + \frac{\partial^3 v_1(\alpha,\lambda)}{\partial \alpha^3} - 6v_1(\alpha,\lambda)\frac{\partial v_1(\alpha,\lambda)}{\partial \alpha} + 3v_2(\alpha,\lambda)\frac{\partial^3 v_2(\alpha,\lambda)}{\partial \alpha^3} + 3\frac{\partial}{\partial \alpha}v_2(\alpha,\lambda)\frac{\partial^2}{\partial \alpha^2}v_2(\alpha,\lambda) \\
&- 3v_2^2(\alpha,\lambda)\frac{\partial v_1(\alpha,\lambda)}{\partial \alpha} + 6v_1(\alpha,\lambda)v_2(\alpha,\lambda)\frac{\partial v_2(\alpha,\lambda)}{\partial \alpha} = 0, \\
&D_{\lambda}^{p} v_2(\alpha,\lambda) + \frac{\partial^3 v_2(\alpha,\lambda)}{\partial \alpha^3} - 3v_2^2(\alpha,\lambda)\frac{\partial v_2(\alpha,\lambda)}{\partial \alpha} - 3v_1(\alpha,\lambda)\frac{\partial v_2(\alpha,\lambda)}{\partial \alpha} + 3v_2(\alpha,\lambda)\frac{\partial v_1(\alpha,\lambda)}{\partial \alpha} = 0, \\
&\lambda > 0, \alpha \in R,\ 0 < p \leq 1
\end{aligned}
\tag{1}
$$

where the spatial coordinate α and the temporal coordinate λ are defined. p is the factor that represents the order of the fractional operator. To investigate this operator, the Caputo form is used. The following changes the fractional coupled system into a classical one when $p = 1$:

$$
\begin{aligned}
&\frac{\partial v_1(\alpha,\lambda)}{\partial \lambda} + \frac{\partial^3 v_1(\alpha,\lambda)}{\partial \alpha^3} - 6v_1(\alpha,\lambda)\frac{\partial v_1(\alpha,\lambda)}{\partial \alpha} + 3v_2(\alpha,\lambda)\frac{\partial^3 v_2(\alpha,\lambda)}{\partial \alpha^3} + 3\frac{\partial}{\partial \alpha}v_2(\alpha,\lambda)\frac{\partial^2}{\partial \alpha^2}v_2(\alpha,\lambda) \\
&- 3v_2^2(\alpha,\lambda)\frac{\partial v_1(\alpha,\lambda)}{\partial \alpha} + 6v_1(\alpha,\lambda)v_2(\alpha,\lambda)\frac{\partial v_2(\alpha,\lambda)}{\partial \alpha} = 0, \\
&\frac{\partial v_2(\alpha,\lambda)}{\partial \lambda} + \frac{\partial^3 v_2(\alpha,\lambda)}{\partial \alpha^3} - 3v_2^2(\alpha,\lambda)\frac{\partial v_2(\alpha,\lambda)}{\partial \alpha} - 3v_1(\alpha,\lambda)\frac{\partial v_2(\alpha,\lambda)}{\partial \alpha} + 3v_2(\alpha,\lambda)\frac{\partial v_1(\alpha,\lambda)}{\partial \alpha} = 0, \\
&\lambda > 0, \alpha \in R,\ 0 < p \leq 1
\end{aligned}
\tag{2}
$$

If $v_2(\alpha,\lambda)$ is equal to zero, the Kersten–Krasil'shchik connected KdV–mKdV system is transformed into the famous KdV system in the following way:

$$
\frac{\partial v_1(\alpha,\lambda)}{\partial \lambda} + \frac{\partial^3 v_1(\alpha,\lambda)}{\partial \alpha^3} - 6v_1(\alpha,\lambda)\frac{\partial v_1(\alpha,\lambda)}{\partial \alpha} = 0,\ \lambda > 0, \alpha \in R,\ 0 < p \leq 1 \tag{3}
$$

At $v_1(\alpha,\lambda) = 0$, the Kersten–Krasil'shchik coupled KdV–mKdV system transforms into the famous mKdV system in the following way:

$$
\frac{\partial v_2(\alpha,\lambda)}{\partial \lambda} + \frac{\partial^3 v_2(\alpha,\lambda)}{\partial \alpha^3} - 3v_2^2(\alpha,\lambda)\frac{\partial v_2(\alpha,\lambda)}{\partial \alpha} = 0,\ \lambda > 0, \alpha \in R,\ 0 < p \leq 1 \tag{4}
$$

This means that the Kersten–Krasil'shchik coupled KdV–mKdV system is just a hybrid of the KdV and mKdV systems, denoted by (1) to (4). Following this, we examine the following third-order KdV system: the fractional nonlinear two-component homogeneous time-fractional coupled system:

$$
\begin{aligned}
&D_{\lambda}^{p} v_1(\alpha,\lambda) - \frac{\partial^3 v_1(\alpha,\lambda)}{\partial \alpha^3} - v_1(\alpha,\lambda)\frac{\partial v_1(\alpha,\lambda)}{\partial \alpha} - v_2(\alpha,\lambda)\frac{\partial v_2(\alpha,\lambda)}{\partial \alpha} = 0,\ \lambda > 0, \alpha \in R,\ 0 < p \leq 1 \\
&D_{\lambda}^{p} v_2(\alpha,\lambda) + 2\frac{\partial^3 v_2(\alpha,\lambda)}{\partial \alpha^3} - v_1(\alpha,\lambda)\frac{\partial v_2(\alpha,\lambda)}{\partial \alpha} = 0,\ \lambda > 0, \alpha \in R,\ 0 < p \leq 1
\end{aligned}
\tag{5}
$$

In this context, λ represents the temporal coordinate, α stands for the spatial coordinate, and p is the order factor of the fractional operator. The Caputo form is used to investigate this operator. The following changes the fractional coupled system into a classical one when $p = 1$:

$$
\begin{aligned}
&\frac{\partial v_1(\alpha,\lambda)}{\partial \lambda} - \frac{\partial^3 v_1(\alpha,\lambda)}{\partial \alpha^3} - v_1(\alpha,\lambda)\frac{\partial v_1(\alpha,\lambda)}{\partial \alpha} - v_2(\alpha,\lambda)\frac{\partial v_2(\alpha,\lambda)}{\partial \alpha} = 0,\ \lambda > 0, \alpha \in R,\ 0 < p \leq 1 \\
&\frac{\partial v_2(\alpha,\lambda)}{\partial \lambda} + 2\frac{\partial^3 v_2(\alpha,\lambda)}{\partial \alpha^3} - v_1(\alpha,\lambda)\frac{\partial v_2(\alpha,\lambda)}{\partial \alpha} = 0,\ \lambda > 0, \alpha \in R,\ 0 < p \leq 1
\end{aligned}
\tag{6}
$$

Omar Abu Arqub created the RPSM in 2013 [20]. The RPSM incorporates the residual error function and Taylor's series and is a semi-analytical method. The convergence series

procedures may be used to solve linear and nonlinear differential equations. Fuzzy DE resolution was the first area to use RPSM in 2013. Arqub et al. [21] created a unique set of RPSM algorithms to find power series solutions for complicated DEs efficiently. Additionally, Arqub et al. [22] developed an appealing new RPSM method that addresses fractional-order nonlinear boundary value problems. El-Ajou et al. [23] created a new RPSM method for estimating solutions to fractional-order KdV–Burgers equations. First, the solution to second- and fourth-order Boussinesq DEs using fractional power series was proposed by Xu et al. [24]. An effective numerical method was created by Zhang et al. [25] by combining RPSM with least square techniques. See references [26–28] for more details.

The researchers used several techniques to resolve fractional-order differential equations (FODEs). The first step is translating the original equation into the Aboodh transform space [29]. Subsequently, distinct solutions to the modified equations are derived. Lastly, the initial equation is solved by using the inverse Aboodh transform. This novel method employs the Sumudu transform in conjunction with homotopy perturbation approaches. The novel power series expansion method solves linear and nonlinear PDEs without linearisation, perturbation, or discretisation. Coefficient computations are much easier than RPSM, where fractional derivatives take many solution iterations. The proposed method, which makes use of a fast convergence series, has the potential to provide a precise closed-form approximation solution.

Aboodh's transform iterative technique (NITM) is the greatest mathematical achievement of the 20th century for fractional partial differential equations. Due to their computational complexity and lack of convergence, partial differential equations with fractional derivatives are challenging to solve using normal approaches. Our innovative method surpasses these limitations by lowering the processing burden, increasing accuracy, and continually improving approximation solutions. Complex mathematical and physical problems have found better solutions via iterations tuned to fractional derivatives [30–34]. Difficult engineering applied mathematics and physics issues may now be studied with the help of defined and understood complex fractional partial differential equation-governed systems.

Two of the most fundamental ways to solve fractional differential equations are the Aboodh transform iterative technique (NITM) and the Aboodh residual power series method (ARPSM). As an additional benefit, these methods provide numerical approximations for solutions to linear and nonlinear differential equations without the need for discretisation or linearisation, in addition to providing instantly accessible symbolic terms of analytical solutions. The primary goal of this research is to find solutions to a system of nonlinear partial differential equations known as the Kersten–Krasil'shchik coupled KdV–mKdV systems utilising two distinct methods: ARPSM and NITM. These two approaches have been combined to solve several nonlinear fractional differential problems.

2. Basic Definitions

Definition 1 ([35]). The function $v(\alpha, \lambda)$ exhibits piecewise continuity and possesses exponential order. The definition of the Aboodh transform for $v(\alpha, \lambda)$ is as follows when $\lambda \geq 0$:

$$A[v(\alpha, \lambda)] = \Psi(\alpha, \nu) = \frac{1}{\nu} \int_0^{\infty} v(\alpha, \lambda) e^{-\lambda \nu} d\lambda, \;\; r_1 \leq \nu \leq r_2.$$

The expression for the inverse Aboodh transform is as follows:

$$A^{-1}[\Psi(\alpha, \nu)] = v(\alpha, \lambda) = \frac{1}{2\pi i} \int_{u-i\infty}^{u+i\infty} \Psi(\alpha, \lambda) \nu e^{\lambda \nu} d\lambda,$$

where $\alpha = (\alpha_1, \alpha_2, \cdots, \alpha_p)$ and $p \in \mathbb{N}$

Lemma 1 ([36,37]). *Consider the functions $v_1(\alpha, \lambda)$ and $v_2(\alpha, \lambda)$, which are piecewise continuous on the interval $[0, \infty[$ and exhibit exponential order, respectively. Assuming that*

$A[v_1(\alpha, \lambda)] = \Psi_1(\alpha, \lambda)$, $A[v_2(\alpha, \lambda)] = \Psi_2(\alpha, \lambda)$ and ϖ_1, ϖ_2 are constants. Therefore, the subsequent statements hold true:

1. $A[\varpi_1 v_1(\alpha,\lambda) + \varpi_2 v_2(\alpha,\lambda)] = \varpi_1 \Psi_1(\alpha,\nu) + \varpi_2 \Psi_2(\alpha,\nu)$;
2. $A^{-1}[\varpi_1 \Psi_1(\alpha,\lambda) + \varpi_2 \Psi_2(\alpha,\lambda)] = \varpi_1 v_1(\alpha,\nu) + \varpi_2 v_2(\alpha,\nu)$;
3. $A[J_\lambda^p v(\alpha,\lambda)] = \frac{\Psi(\alpha,\nu)}{\nu^p}$;
4. $A[D_\lambda^p v(\alpha,\lambda)] = \nu^p \Psi(\alpha,\nu) - \sum_{K=0}^{r-1} \frac{v^K(\alpha,0)}{\nu^{K-p+2}}, r-1 < p \leq r,\ r \in \mathbb{N}$.

Definition 2 ([38]). The definition of the fractional derivative of a function $v(\alpha,\lambda)$ of order p is as follows, adhering to the Caputo sense:

$$D_\lambda^p v(\alpha,\lambda) = J_\lambda^{m-p} v^{(m)}(\alpha,\lambda),\ r \geq 0,\ m-1 < p \leq m,$$

where $\alpha = (\alpha_1, \alpha_2, \cdots, \alpha_p) \in \mathbb{R}^p$ and $m, p \in R$, J_λ^{m-p} is the R–L integral of $v(\alpha,\lambda)$.

Definition 3 ([39]). The expression for the power series is:

$$\sum_{r=0}^{\infty} \hbar_r(\alpha)(\lambda-\lambda_0)^{rp} = \hbar_0(\lambda-\lambda_0)^0 + \hbar_1(\lambda-\lambda_0)^p + \hbar_2(\lambda-\lambda_0)^{2p} + \cdots,$$

where $p \in \mathbb{N}$ and $\alpha = (\alpha_1, \alpha_2, \cdots, \alpha_p) \in \mathbb{R}^p$. This series is recognised as a multiple fractional power series (MFPS) around λ_0, where $\hbar_r(\alpha)$ represents the series coefficients and λ is a variable.

Lemma 2. *Assuming that the function $v(\alpha,\lambda)$ is an exponential order, the Aboodh transform is denoted as $A[v(\alpha,\lambda)] = \Psi(\alpha,\nu)$. Consequently,*

$$A[D_\lambda^{rp} v(\alpha,\lambda)] = \nu^{rp}\Psi(\alpha,\nu) - \sum_{j=0}^{r-1} \nu^{p(r-j)-2} D_\lambda^{jp} v(\alpha,0), 0 < p \leq 1, \tag{7}$$

where $\alpha = (\alpha_1, \alpha_2, \cdots, \alpha_p) \in \mathbb{R}^p$ and $p \in \mathbb{N}$ and $D_\lambda^{rp} = D_\lambda^p . D_\lambda^p . \cdots . D_\lambda^p (r - times)$.

Proof. To confirm Equation (2), let us employ the method of induction. Substituting $r = 1$ into Equation (2) produces the following outcome:

$$A[D_\lambda^{2p} v(\alpha,\lambda)] = \nu^{2p}\Psi(\alpha,\nu) - \nu^{2p-2} v(\alpha,0) - \nu^{p-2} D_\lambda^p v(\alpha,0).$$

The equation's validity for $r = 1$ is substantiated by Part (4) of Lemma 1. By substituting $r = 2$ into Equation (2), we obtain:

$$A[D_r^{2p} v(\alpha,\lambda)] = \nu^{2p}\Psi(\alpha,\nu) - \nu^{2p-2} v(\alpha,0) - \nu^{p-2} D_\lambda^p v(\alpha,0). \tag{8}$$

Considering the left-hand side (L.H.S.) of Equation (8), we obtain

$$L.H.S = A[D_\lambda^{2p} v(\alpha,\lambda)]. \tag{9}$$

There exists a particular manner to express Equation (9) as

$$L.H.S = A[D_\lambda^p v(\alpha,\lambda)]. \tag{10}$$

Let

$$z(\alpha,\lambda) = D_\lambda^p v(\alpha,\lambda). \tag{11}$$

Hence, Equation (10) transforms to

$$L.H.S = A[D_\lambda^p z(\alpha,\lambda)]. \tag{12}$$

The fractional Caputo-type derivative is defined as

$$L.H.S = A[J^{1-p} z'(\alpha,\lambda)]. \tag{13}$$

Equation (13) presents the R–L fractional integral formula for the Aboodh transform.

$$L.H.S = \frac{A[z^{'}(\alpha,\lambda)]}{\nu^{1-p}}. \tag{14}$$

Utilising the differential property of the Aboodh transform, Equation (14) is altered to

$$L.H.S = \nu^{p} Z(\alpha,\nu) - \frac{z(\alpha,0)}{\nu^{2-p}}. \tag{15}$$

Referring to Equation (11), we derive

$$Z(\alpha,\nu) = \nu^{p}\Psi(\alpha,\nu) - \frac{v(\alpha,0)}{\nu^{2-p}},$$

where $A[z(\alpha,\lambda)] = Z(\alpha,\nu)$. As a result, Equation (15) is transformed into

$$L.H.S = \nu^{2p}\Psi(\alpha,\nu) - \frac{v(\alpha,0)}{\nu^{2-2p}} - \frac{D_{\lambda}^{p} v(\alpha,0)}{\nu^{2-p}}. \tag{16}$$

Equations (2) and (16) exhibit compatibility. Assuming $r = K$ holds true for Equation (2). Consequently, substitute $r = K$ into Equation (2):

$$A[D_{\lambda}^{Kp} v(\alpha,\lambda)] = \nu^{Kp}\Psi(\alpha,\nu) - \sum_{j=0}^{K-1} \nu^{p(K-j)-2} D_{\lambda}^{jp} D_{\lambda}^{jp} v(\alpha,0),\ 0 < p \leq 1. \tag{17}$$

Below, we will demonstrate the validity of Equation (2) for $r = K+1$:

$$A[D_{\lambda}^{(K+1)p} v(\alpha,\lambda)] = \nu^{(K+1)p}\Psi(\alpha,\nu) - \sum_{j=0}^{K} \nu^{p((K+1)-j)-2} D_{\lambda}^{jp} v(\alpha,0). \tag{18}$$

On the left-hand side of Equation (18), we obtain

$$L.H.S = A[D_{\lambda}^{Kp}(D_{\lambda}^{Kp})]. \tag{19}$$

Assume

$$D_{\lambda}^{Kp} = g(\alpha,\lambda).$$

Equation (19) gives us

$$L.H.S = A[D_{\lambda}^{p} g(\alpha,\lambda)]. \tag{20}$$

Equation (20) can be formulated utilising the Caputo fractional derivative and the R–L integral formula.

$$L.H.S = \nu^{p} A[D_{\lambda}^{Kp} v(\alpha,\lambda)] - \frac{g(\alpha,0)}{\nu^{2-p}}. \tag{21}$$

Utilising Equation (17), (21) is altered into

$$L.H.S = \nu^{rp}\Psi(\alpha,\nu) - \sum_{j=0}^{r-1} \nu^{p(r-j)-2} D_{\lambda}^{jp} v(\alpha,0). \tag{22}$$

By using Equation (22), we have the following result:

$$L.H.S = A[D_{\lambda}^{rp} v(\alpha,0)].$$

For $r = K+1$, this implies the validity of Equation (2). Hence, the mathematical induction technique was employed to establish the validity of Equation (2) for all positive integers.

In the following lemma, we present a revised version of the ARPSM multiple fractional Taylor's formula. □

Lemma 3. *Let $v(\alpha,\lambda)$ be an exponentially ordered function. $A[v(\alpha,\lambda)] = \Psi(\alpha,\nu)$ is the Aboodh transform of $v(\alpha,\lambda)$ as a multiple fractional Taylor's series:*

$$\Psi(\alpha,\nu)=\sum_{r=0}^{\infty}\frac{\hbar_r(\alpha)}{\nu^{rp+2}},\nu>0, \tag{23}$$

where $\alpha=(\alpha_1,\alpha_2,\cdots,\alpha_p)\in\mathbb{R}^p,\ p\in\mathbb{N}$.

Proof. Following Taylor's series fractional order analysis, we obtain

$$v(\alpha,\lambda)=\hbar_0(\alpha)+\hbar_1(\alpha)\frac{\lambda^p}{\Gamma[p+1]}++\hbar_2(\alpha)\frac{\lambda^{2p}}{\Gamma[2p+1]}+\cdots. \tag{24}$$

Equation (24) can be transformed using the Aboodh transform to yield the following equality:

$$A[v(\alpha,\lambda)]=A[\hbar_0(\alpha)]+A\left[\hbar_1(\alpha)\frac{\lambda^p}{\Gamma[p+1]}\right]+A\left[\hbar_1(\alpha)\frac{\lambda^{2p}}{\Gamma[2p+1]}\right]+\cdots$$

Using these features of the Aboodh transform, we derive

$$A[v(\alpha,\lambda)]=\hbar_0(\alpha)\frac{1}{\nu^2}+\hbar_1(\alpha)\frac{\Gamma[p+1]}{\Gamma[p+1]}\frac{1}{\nu^{p+2}}+\hbar_2(\alpha)\frac{\Gamma[2p+1]}{\Gamma[2p+1]}\frac{1}{\nu^{2p+2}}\cdots$$

Consequently, we derive (23), a novel Taylor's series in the Aboodh transform. □

Lemma 4. *Assume that the function $A[v(\alpha,\lambda)]=\Psi(\alpha,\nu)$ has an MFPS representation in the new form of Taylor's series (23):*

$$\hbar_0(\alpha)=\lim_{\nu\to\infty}\nu^2\Psi(\alpha,\nu)=v(\alpha,0). \tag{25}$$

Proof. The previous equation is based on an updated version of Taylor's series.

$$\hbar_0(\alpha)=\nu^2\Psi(\alpha,\nu)-\frac{\hbar_1(\alpha)}{\nu^p}-\frac{\hbar_2(\alpha)}{\nu^{2p}}-\cdots \tag{26}$$

Through the use of $\lim_{\nu\to\infty}$ to Equation (26) and some computation, the desired outcome, denoted by (25), is obtained. □

Theorem 1. *The function $v(\alpha,\lambda)$ and $\Psi(\alpha,\nu)$ have the following MFPS representations:*

$$\Psi(\alpha,\nu)=\sum_{0}^{\infty}\frac{\hbar_r(\alpha)}{\nu^{rp+2}},\ \nu>0,$$

where $\alpha=(\alpha_1,\alpha_2,\cdots,\alpha_p)\in\mathbb{R}^p$ and $p\in\mathbb{N}$. Then, we have

$$\hbar_r(\alpha)=D_r^{rp}v(\alpha,0),$$

where $D_\lambda^{rp}=D_\lambda^p.D_\lambda^p.\cdots.D_\lambda^p(r-times)$.

Proof. The revised Taylor's series form gives us

$$\hbar_1(\alpha)=\nu^{p+2}\Psi(\alpha,\nu)-\nu^p\hbar_0(\alpha)-\frac{\hbar_2(\alpha)}{\nu^p}-\frac{\hbar_3(\alpha)}{\nu^{2p}}-\cdots \tag{27}$$

Equation (27) for $\lim_{\nu\to\infty}$ may be solved to obtain

$$\hbar_1(\alpha)=\lim_{\nu\to\infty}(\nu^{p+2}\Psi(\alpha,\nu)-\nu^p\hbar_0(\alpha))-\lim_{\nu\to\infty}\frac{\hbar_2(\alpha)}{\nu^p}-\lim_{\nu\to\infty}\frac{\hbar_3(\alpha)}{\nu^{2p}}-\cdots$$

Taking the limit leads to the following equality:

$$\hbar_1(\alpha)=\lim_{\nu\to\infty}(\nu^{p+2}\Psi(\alpha,\nu)-\nu^p\hbar_0(\alpha)). \tag{28}$$

Lemma 2 in combination with Equation (28) yields the following outcome:

$$\hbar_1(\alpha) = \lim_{\nu\to\infty}(\nu^2 A[D_\lambda^p v(\alpha,\lambda)](\nu)). \tag{29}$$

Furthermore, when applying Equation (29) together with Lemma 3, the outcome is

$$\hbar_1(\alpha) = D_\lambda^p v(\alpha,0).$$

Using the modified Taylor's series along with $\nu \to \infty$, we obtain

$$\hbar_2(\alpha) = \nu^{2p+2}\Psi(\alpha,\nu) - \nu^{2p}\hbar_0(\alpha) - \nu^p\hbar_1(\alpha) - \frac{\hbar_3(\alpha)}{\nu^p} - \cdots$$

Using Lemma 3, we obtain

$$\hbar_2(\alpha) = \lim_{\nu\to\infty}\nu^2(\nu^{2p}\Psi(\alpha,\nu) - \nu^{2p-2}\hbar_0(\alpha) - \nu^{p-2}\hbar_1(\alpha)). \tag{30}$$

Lemmas 2 and 4 are used again to transform Equation (30):

$$\hbar_2(\alpha) = D_\lambda^{2p} v(\alpha,0).$$

Using the same procedure on the modified version of Taylor's series, we obtain

$$\hbar_3(\alpha) = \lim_{\nu\to\infty}\nu^2(A[D_\lambda^{2p} v(\alpha,p)](\nu)).$$

Lemma 4 is applied to obtain the final equation:

$$\hbar_3(\alpha) = D_\lambda^{3p} v(\alpha,0).$$

In general, we obtain

$$\hbar_r(\alpha) = D_\lambda^{rp} v(\alpha,0).$$

Thus, the proof is ended. □

In the following theorem, we demonstrate the necessary and sufficient conditions for the modified Taylor formula to converge.

Theorem 2. *Lemma 3 presents a revised multiple fractional Taylor's formula, represented as* $A[v(\alpha,\lambda)] = \Psi(\alpha,\nu)$. *If* $|\nu^a A[D_\lambda^{(K+1)p} v(\alpha,\lambda)]| \le T$, *then the updated multiple fractional Taylor's formula for* $(0\ \nu \le s)$ *with* $0\ p \le 1$ *aligns with the subsequent inequality:*

$$|R_K(\alpha,\nu)| \le \frac{T}{\nu^{(K=1)p+2}},\ 0 < \nu \le s.$$

Proof. To begin the proof, we start with the following assumptions:

$A[D_\lambda^{rp} v(\alpha,\lambda)]$ is defined for $0 < \nu \le s$, where $r = 0,1,2,\cdots,K+1$. Assume $|\nu^2 A[D_{\lambda^{K+1}} v(\alpha,\tau)]| \le T$ holds for $0 < \nu \le s$ given the specified conditions. Examine the resultant relationship derived from Taylor's series in its updated format:

$$R_K(\alpha,\nu) = \Psi(\alpha,\nu) - \sum_{r=0}^{K}\frac{\hbar_r(\alpha)}{\nu^{rp+2}}. \tag{31}$$

If Theorem 1 is employed, Equation (31) transforms to:

$$R_K(\alpha,\nu) = \Psi(\alpha,\nu) - \sum_{r=0}^{K}\frac{D_\lambda^{rp} v(\alpha,0)}{\nu^{rp+2}}. \tag{32}$$

Multiply both sides of Equation (32) by $\nu^{(K+1)a+2}$. Considering that:

$$\nu^{(K+1)p+2}R_K(\alpha,\nu) = \nu^2(\nu^{(K+1)p}\Psi(\alpha,\nu) - \sum_{r=0}^{K}\nu^{(K+1-r)p-2}D_\lambda^{rp} v(\alpha,0)). \tag{33}$$

Utilising Lemma 2 on Equation (33) results in:

$$\nu^{(K+1)p+2}R_K(\alpha,\nu) = \nu^2 A[D_\lambda^{(K+1)p}v(\alpha,\lambda)]. \tag{34}$$

Taking the absolute of Equation (34) results in:

$$|\nu^{(K+1)p+2}R_K(\alpha,\nu)| = |\nu^2 A[D_\lambda^{(K+1)p}v(\alpha,\lambda)]|. \tag{35}$$

Implementing the condition specified in Equation (35) leads to the subsequent conclusion, thus:

$$\frac{-T}{\nu^{(K+1)p+2}} \leq R_K(\alpha,\nu) \leq \frac{T}{\nu^{(K+1)p+2}}. \tag{36}$$

Equation (36) leads to the desired outcome.

$$|R_K(\alpha,\nu)| \leq \frac{T}{\nu^{(K+1)p+2}}.$$

Consequently, the convergence condition for the new series is established. □

3. Outline Detailing the Suggested Methodologies

3.1. The ARPSM Technique for Addressing Time-Fractional Partial Differential Equations with Varied Coefficients

We present the guiding principles of ARPSM to address our general model.

Step 1: Write the equation in general form.

$$D_\lambda^{qp}v(\alpha,\lambda) + \vartheta(\alpha)N(v) - \alpha(\alpha,v) = 0 \tag{37}$$

Step 2: Utilising the Aboodh transformation on both sides of Equation (37) yields:

$$A[D_\lambda^{qp}v(\alpha,\lambda) + \vartheta(\alpha)N(v) - \alpha(\alpha,v)] = 0 \tag{38}$$

Let us transform Equation (38) by employing Lemma 2:

$$\Psi(\alpha,s) = \sum_{j=0}^{q-1}\frac{D_\lambda^j v(\alpha,0)}{s^{qp+2}} - \frac{\vartheta(\alpha)Y(s)}{s^{qp}} + \frac{F(\alpha,s)}{s^{qp}}, \tag{39}$$

where $A[\alpha(\alpha,v)] = F(\alpha,s)$, $A[N(v)] = Y(s)$.

Step 3: In order to obtain the solution to Equation (39), consider the form:

$$\Psi(\alpha,s) = \sum_{r=0}^{\infty}\frac{\hbar_r(\alpha)}{s^{rp+2}},\ s>0$$

Step 4: Proceed with the following steps:

$$\hbar_0(\alpha) = \lim_{s\to\infty} s^2\Psi(\alpha,s) = v(\alpha,0)$$

Utilising Theorem 2, the following result is obtained:

$$\hbar_1(\alpha) = D_\lambda^p v(\alpha,0),$$

$$\hbar_2(\alpha) = D_\lambda^{2p} v(\alpha,0),$$

$$\vdots$$

$$\hbar_w(\alpha) = D_\lambda^{wp} v(\alpha,0).$$

Step 5: Obtain $\Psi(\alpha,s)$ as the K^{th}-truncated series by following these outlined steps:

$$\Psi_K(\alpha,s) = \sum_{r=0}^{K}\frac{\hbar_r(\alpha)}{s^{rp+2}},\ s>0,$$

$$\Psi_K(\alpha,s)=\frac{\hbar_0(\alpha)}{s^2}+\frac{\hbar_1(\alpha)}{s^{p+2}}+\cdots+\frac{\hbar_w(\alpha)}{s^{wp+2}}+\sum_{r=w+1}^{K}\frac{\hbar_r(\alpha)}{s^{rp+2}}.$$

Step 6: The evaluation of the Aboodh residual function (ARF) of Equation (39) must be conducted distinctly from the K^{th}-truncated Aboodh residual function in order to obtain:

$$ARes(\alpha,s)=\Psi(\alpha,s)-\sum_{j=0}^{q-1}\frac{D_\lambda^j v(\alpha,0)}{s^{jp+2}}+\frac{\vartheta(\alpha)Y(s)}{s^{jp}}-\frac{F(\alpha,s)}{s^{jp}},$$

and

$$ARes_K(\alpha,s)=\Psi_K(\alpha,s)-\sum_{j=0}^{q-1}\frac{D_\lambda^j v(\alpha,0)}{s^{jp+2}}+\frac{\vartheta(\alpha)Y(s)}{s^{jp}}-\frac{F(\alpha,s)}{s^{jp}}. \tag{40}$$

Step 7: Substitute the expansion form of $\Psi_K(\alpha,s)$ into Equation (40).

$$\begin{aligned}ARes_K(\alpha,s)=&\Big(\frac{\hbar_0(\alpha)}{s^2}+\frac{\hbar_1(\alpha)}{s^{p+2}}+\cdots+\frac{\hbar_w(\alpha)}{s^{wp+2}}+\sum_{r=w+1}^{K}\frac{\hbar_r(\alpha)}{s^{rp+2}}\Big)\\&-\sum_{j=0}^{q-1}\frac{D_\lambda^j v(\alpha,0)}{s^{jp+2}}+\frac{\vartheta(\alpha)Y(s)}{s^{jp}}-\frac{F(\alpha,s)}{s^{jp}}.\end{aligned} \tag{41}$$

Step 8: Multiply both sides of Equation (41) by s^{Kp+2}.

$$\begin{aligned}s^{Kp+2}ARes_K(\alpha,s)=&s^{Kp+2}\Big(\frac{\hbar_0(\alpha)}{s^2}+\frac{\hbar_1(\alpha)}{s^{p+2}}+\cdots+\frac{\hbar_w(\alpha)}{s^{wp+2}}+\sum_{r=w+1}^{K}\frac{\hbar_r(\alpha)}{s^{rp+2}}\\&-\sum_{j=0}^{q-1}\frac{D_\lambda^j v(\alpha,0)}{s^{jp+2}}+\frac{\vartheta(\alpha)Y(s)}{s^{jp}}-\frac{F(\alpha,s)}{s^{jp}}\Big).\end{aligned} \tag{42}$$

Step 9: Both sides of Equation (42) are then evaluated with respect to $\lim_{s\to\infty}$.

$$\begin{aligned}\lim_{s\to\infty}s^{Kp+2}ARes_K(\alpha,s)=&\lim_{s\to\infty}s^{Kp+2}\Big(\frac{\hbar_0(\alpha)}{s^2}+\frac{\hbar_1(\alpha)}{s^{p+2}}+\cdots+\frac{\hbar_w(\alpha)}{s^{wp+2}}+\sum_{r=w+1}^{K}\frac{\hbar_r(\alpha)}{s^{rp+2}}\\&-\sum_{j=0}^{q-1}\frac{D_\lambda^j v(\alpha,0)}{s^{jp+2}}+\frac{\vartheta(\alpha)Y(s)}{s^{jp}}-\frac{F(\alpha,s)}{s^{jp}}\Big).\end{aligned}$$

Step 10: In order to obtain $\hbar_K(\alpha)$, it is necessary to solve the subsequent equation:

$$\lim_{s\to\infty}(s^{Kp+2}ARes_K(\alpha,s))=0,$$

where $K=w+1,w+2,\cdots$.
Step 11: The K-approximate solution for Equation (39) can be obtained by substituting the values of $\hbar_K(\alpha)$ into the K-truncated series of $\Psi(\alpha,s)$.
Step 12: Applying an inverse Aboodh transform to $\Psi_K(\alpha,s)$ might yield the K-approximate solution $v_K(\alpha,\lambda)$.

3.2. Problem 1

Let us analyze the combined fractional Kersten–Krasil'shchik KdV–mKdV nonlinear system as presented below:

$$\begin{aligned}&D_\lambda^p v_1(\alpha,\lambda)+\frac{\partial^3 v_1(\alpha,\lambda)}{\partial\alpha^3}-6v_1(\alpha,\lambda)\frac{\partial v_1(\alpha,\lambda)}{\partial\alpha}+3v_2(\alpha,\lambda)\frac{\partial^3 v_2(\alpha,\lambda)}{\partial\alpha^3}+3\frac{\partial}{\partial\alpha}v_2(\alpha,\lambda)\frac{\partial^2}{\partial\alpha^2}v_2(\alpha,\lambda)\\&-3v_2^2(\alpha,\lambda)\frac{\partial v_1(\alpha,\lambda)}{\partial\alpha}+6v_1(\alpha,\lambda)v_2(\alpha,\lambda)\frac{\partial v_2(\alpha,\lambda)}{\partial\alpha}=0,\end{aligned} \tag{43}$$

$$D_\lambda^p v_2(\alpha,\lambda) + \frac{\partial^3 v_2(\alpha,\lambda)}{\partial\alpha^3} - 3v_2^2(\alpha,\lambda)\frac{\partial v_2(\alpha,\lambda)}{\partial\alpha} - 3v_1(\alpha,\lambda)\frac{\partial v_2(\alpha,\lambda)}{\partial\alpha} + 3v_2(\alpha,\lambda)\frac{\partial v_1(\alpha,\lambda)}{\partial\alpha} = 0, \quad (44)$$

where $0 < p \leq 1$.

With the following IC's:

$$v_1(\alpha,0) = c - 2c\,\mathrm{sech}^2\left(\sqrt{c}\alpha\right), \quad (45)$$

$$v_2(\alpha,0) = 2\sqrt{c}\,\mathrm{sech}\left(\sqrt{c}\alpha\right), \quad (46)$$

and exact solution

$$v_1(\alpha,0) = c - 2c\,\mathrm{sech}^2\left(\sqrt{c}(2c\lambda+\alpha)\right), \quad (47)$$

$$v_2(\alpha,0) = 2\sqrt{c}\,\mathrm{sech}\left(\sqrt{c}(2c\lambda+\alpha)\right). \quad (48)$$

Equations (45) and (46) are employed, and utilising the Aboodh Transform (AT) on Equations (43) and (44), we obtain:

$$\begin{aligned} &v_1(\alpha,t) - \frac{c-2c\,\mathrm{sech}^2\left(\sqrt{c}\alpha\right)}{s^2} + \frac{1}{s^p}\mathcal{A}_\lambda\left[\frac{\partial^3\mathcal{A}_\lambda^{-1}v_1(\alpha,\lambda)}{\partial\alpha^3}\right] - \frac{6}{s^p}\mathcal{A}_\lambda\left[\mathcal{A}_\lambda^{-1}v_1(\alpha,\lambda)\frac{\partial\mathcal{A}_\lambda^{-1}v_1(\alpha,\lambda)}{\partial\alpha}\right] \\ &+ \frac{3}{s^p}\mathcal{A}_\lambda\left[\mathcal{A}_\lambda^{-1}v_2(\alpha,\lambda)\frac{\partial^3\mathcal{A}_\lambda^{-1}v_2(\alpha,\lambda)}{\partial\alpha^3}\right] + \frac{3}{s^p}\mathcal{A}_\lambda\left[\frac{\partial}{\partial\alpha}\mathcal{A}_\lambda^{-1}v_2(\alpha,\lambda)\frac{\partial^2}{\partial\alpha^2}\mathcal{A}_\lambda^{-1}v_2(\alpha,\lambda)\right] \\ &- \frac{3}{s^p}\mathcal{A}_\lambda\left[\mathcal{A}_\lambda^{-1}v_2^2(\alpha,\lambda)\frac{\partial\mathcal{A}_\lambda^{-1}v_1(\alpha,\lambda)}{\partial\alpha}\right] + \frac{6}{s^p}\mathcal{A}_\lambda\left[\mathcal{A}_\lambda^{-1}v_1(\alpha,\lambda)\mathcal{A}_\lambda^{-1}v_2(\alpha,\lambda)\frac{\partial\mathcal{A}_\lambda^{-1}v_2(\alpha,\lambda)}{\partial\alpha}\right] = 0, \end{aligned} \quad (49)$$

$$\begin{aligned} &v_2(\alpha,t) - \frac{2\sqrt{c}\,\mathrm{sech}\left(\sqrt{c}\alpha\right)}{s^2} + \frac{1}{s^p}\mathcal{A}_\lambda\left[\frac{\partial^3\mathcal{A}_\lambda^{-1}v_2(\alpha,\lambda)}{\partial\alpha^3}\right] - \frac{3}{s^p}\mathcal{A}_\lambda\left[\mathcal{A}_\lambda^{-1}v_2^2(\alpha,\lambda)\frac{\partial\mathcal{A}_\lambda^{-1}v_2(\alpha,\lambda)}{\partial\alpha}\right] \\ &- \frac{3}{s^p}\mathcal{A}_\lambda\left[\mathcal{A}_\lambda^{-1}v_1(\alpha,\lambda)\frac{\partial\mathcal{A}_\lambda^{-1}v_2(\alpha,\lambda)}{\partial\alpha}\right] + \frac{3}{s^p}\mathcal{A}_\lambda\left[\mathcal{A}_\lambda^{-1}v_2(\alpha,\lambda)\frac{\partial\mathcal{A}_\lambda^{-1}v_1(\alpha,\lambda)}{\partial\alpha}\right] = 0. \end{aligned} \quad (50)$$

Hence, the term series that have been k^{th} truncated are

$$v_1(\alpha,s) = \frac{c-2c\,\mathrm{sech}^2\left(\sqrt{c}\alpha\right)}{s^2} + \sum_{r=1}^{k}\frac{f_r(\alpha,s)}{s^{rp+1}}, \quad r = 1,2,3,4\cdots. \quad (51)$$

$$v_2(\alpha,s) = \frac{2\sqrt{c}\,\mathrm{sech}\left(\sqrt{c}\alpha\right)}{s^2} + \sum_{r=1}^{k}\frac{g_r(\alpha,s)}{s^{rp+1}}, \quad r = 1,2,3,4\cdots. \quad (52)$$

Aboodh residual functions (ARFs) are

$$\begin{aligned} &\mathcal{A}_\lambda Res(\alpha,s) = v_1(\alpha,t) - \frac{c-2c\,\mathrm{sech}^2\left(\sqrt{c}\alpha\right)}{s^2} + \frac{1}{s^p}\mathcal{A}_\lambda\left[\frac{\partial^3\mathcal{A}_\lambda^{-1}v_1(\alpha,\lambda)}{\partial\alpha^3}\right] - \frac{6}{s^p}\mathcal{A}_\lambda\left[\mathcal{A}_\lambda^{-1}v_1(\alpha,\lambda)\frac{\partial\mathcal{A}_\lambda^{-1}v_1(\alpha,\lambda)}{\partial\alpha}\right] \\ &+ \frac{3}{s^p}\mathcal{A}_\lambda\left[\mathcal{A}_\lambda^{-1}v_2(\alpha,\lambda)\frac{\partial^3\mathcal{A}_\lambda^{-1}v_2(\alpha,\lambda)}{\partial\alpha^3}\right] + \frac{3}{s^p}\mathcal{A}_\lambda\left[\frac{\partial}{\partial\alpha}\mathcal{A}_\lambda^{-1}v_2(\alpha,\lambda)\frac{\partial^2}{\partial\alpha^2}\mathcal{A}_\lambda^{-1}v_2(\alpha,\lambda)\right] \\ &- \frac{3}{s^p}\mathcal{A}_\lambda\left[\mathcal{A}_\lambda^{-1}v_2^2(\alpha,\lambda)\frac{\partial\mathcal{A}_\lambda^{-1}v_1(\alpha,\lambda)}{\partial\alpha}\right] + \frac{6}{s^p}\mathcal{A}_\lambda\left[\mathcal{A}_\lambda^{-1}v_1(\alpha,\lambda)\mathcal{A}_\lambda^{-1}v_2(\alpha,\lambda)\frac{\partial\mathcal{A}_\lambda^{-1}v_2(\alpha,\lambda)}{\partial\alpha}\right] = 0 \end{aligned} \quad (53)$$

$$\begin{aligned}\mathcal{A}_\lambda Res(\alpha,s) &= v_2(\alpha,t) - \frac{2\sqrt{c}\,\mathrm{sech}\left(\sqrt{c}\alpha\right)}{s^2} + \frac{1}{s^p}\mathcal{A}_\lambda\left[\frac{\partial^3\mathcal{A}_\lambda^{-1}v_2(\alpha,\lambda)}{\partial\alpha^3}\right] - \frac{3}{s^p}\mathcal{A}_\lambda\left[\mathcal{A}_\lambda^{-1}v_2^2(\alpha,\lambda)\frac{\partial\mathcal{A}_\lambda^{-1}v_2(\alpha,\lambda)}{\partial\alpha}\right]\\ &- \frac{3}{s^p}\mathcal{A}_\lambda\left[\mathcal{A}_\lambda^{-1}v_1(\alpha,\lambda)\frac{\partial\mathcal{A}_\lambda^{-1}v_2(\alpha,\lambda)}{\partial\alpha}\right] + \frac{3}{s^p}\mathcal{A}_\lambda\left[\mathcal{A}_\lambda^{-1}v_2(\alpha,\lambda)\frac{\partial\mathcal{A}_\lambda^{-1}v_1(\alpha,\lambda)}{\partial\alpha}\right] = 0\end{aligned} \tag{54}$$

and the k^{th}-LRFs as:

$$\begin{aligned}\mathcal{A}_\lambda Res_k(\alpha,s) &= v_{1,k}(\alpha,t) - \frac{c-2c\,\mathrm{sech}^2\left(\sqrt{c}\alpha\right)}{s^2} + \frac{1}{s^p}\mathcal{A}_\lambda\left[\frac{\partial^3\mathcal{A}_\lambda^{-1}v_{1,k}(\alpha,\lambda)}{\partial\alpha^3}\right] - \frac{6}{s^p}\mathcal{A}_\lambda\left[\mathcal{A}_\lambda^{-1}v_{1,k}(\alpha,\lambda)\frac{\partial\mathcal{A}_\lambda^{-1}v_{1,k}(\alpha,\lambda)}{\partial\alpha}\right]\\ &+ \frac{3}{s^p}\mathcal{A}_\lambda\left[\mathcal{A}_\lambda^{-1}v_{2,k}(\alpha,\lambda)\frac{\partial^3\mathcal{A}_\lambda^{-1}v_{2,k}(\alpha,\lambda)}{\partial\alpha^3}\right] + \frac{3}{s^p}\mathcal{A}_\lambda\left[\frac{\partial}{\partial\alpha}\mathcal{A}_\lambda^{-1}v_{2,k}(\alpha,\lambda)\frac{\partial^2}{\partial\alpha^2}\mathcal{A}_\lambda^{-1}v_{2,k}(\alpha,\lambda)\right]\\ &- \frac{3}{s^p}\mathcal{A}_\lambda\left[\mathcal{A}_\lambda^{-1}v_{2,k}^2(\alpha,\lambda)\frac{\partial\mathcal{A}_\lambda^{-1}v_{1,k}(\alpha,\lambda)}{\partial\alpha}\right] + \frac{6}{s^p}\mathcal{A}_\lambda\left[\mathcal{A}_\lambda^{-1}v_{1,k}(\alpha,\lambda)\mathcal{A}_\lambda^{-1}v_{2,k}(\alpha,\lambda)\frac{\partial\mathcal{A}_\lambda^{-1}v_{2,k}(\alpha,\lambda)}{\partial\alpha}\right] = 0\end{aligned} \tag{55}$$

$$\begin{aligned}\mathcal{A}_\lambda Res_k(\alpha,s) &= v_{2,k}(\alpha,t) - \frac{2\sqrt{c}\,\mathrm{sech}\left(\sqrt{c}\alpha\right)}{s^2} + \frac{1}{s^p}\mathcal{A}_\lambda\left[\frac{\partial^3\mathcal{A}_\lambda^{-1}v_{2,k}(\alpha,\lambda)}{\partial\alpha^3}\right] - \frac{3}{s^p}\mathcal{A}_\lambda\left[\mathcal{A}_\lambda^{-1}v_{2,k}^2(\alpha,\lambda)\frac{\partial\mathcal{A}_\lambda^{-1}v_{2,k}(\alpha,\lambda)}{\partial\alpha}\right]\\ &- \frac{3}{s^p}\mathcal{A}_\lambda\left[\mathcal{A}_\lambda^{-1}v_{1,k}(\alpha,\lambda)\frac{\partial\mathcal{A}_\lambda^{-1}v_{2,k}(\alpha,\lambda)}{\partial\alpha}\right] + \frac{3}{s^p}\mathcal{A}_\lambda\left[\mathcal{A}_\lambda^{-1}v_{2,k}(\alpha,\lambda)\frac{\partial\mathcal{A}_\lambda^{-1}v_{1,k}(\alpha,\lambda)}{\partial\alpha}\right] = 0\end{aligned} \tag{56}$$

To compute $f_r(\alpha,s)$ and $g_r(\alpha,s)$, follow these steps: multiply the resulting equations by s^{rp+1} and substitute the r^{th}-truncated series from Equations (51) and (52) into the r^{th}-Aboodh residual function represented by Equations (55) and (56). Then, iteratively solve the relations $\lim_{s\to\infty}(s^{rp+1}A\lambda Resv_1,r(\alpha,s)) = 0$ and $\lim_{s\to\infty}(s^{rp+1}A\lambda Resv_2,r(\alpha,s)) = 0$ for $r = 1,2,3,\cdots$. The first few terms are as follows:

$$\begin{aligned}f_1(\alpha,s) &= 4c^{5/2}\left(7\cosh\left(2\sqrt{c}\alpha\right) - 17\right)\tanh\left(\sqrt{c}\alpha\right)\mathrm{sech}^4\left(\sqrt{c}\alpha\right),\\ g_1(\alpha,s) &= -c^2\left(49\sinh\left(\sqrt{c}\alpha\right) + \sinh\left(3\sqrt{c}\alpha\right)\right)\mathrm{sech}^4\left(\sqrt{c}\alpha\right),\end{aligned} \tag{57}$$

$$\begin{aligned}f_2(\alpha,s) &= -c^4\left(-29013\cosh\left(2\sqrt{c}\alpha\right) + 2112\cosh\left(4\sqrt{c}\alpha\right) + 13\cosh\left(6\sqrt{c}\alpha\right) + 32248\right)\mathrm{sech}^8\left(\sqrt{c}\alpha\right),\\ g_2(\alpha,s) &= \frac{1}{4}c^{7/2}\left(11119\cosh\left(2\sqrt{c}\alpha\right) - 146\cosh\left(4\sqrt{c}\alpha\right) + \cosh\left(6\sqrt{c}\alpha\right) - 14078\right)\mathrm{sech}^7\left(\sqrt{c}\alpha\right),\end{aligned} \tag{58}$$

and so on.

Putting the values of $f_r(\alpha,s)$ and $g_r(\alpha,s)$, $r = 1,2,3,\cdots$, in Equations (51) and (52), we obtain

$$\begin{aligned}v_1(\alpha,s) &= \frac{4c^{5/2}\left(7\cosh\left(2\sqrt{c}\alpha\right) - 17\right)\tanh\left(\sqrt{c}\alpha\right)\mathrm{sech}^4\left(\sqrt{c}\alpha\right)}{s^{\lambda+1}}\\ &- \frac{c^4\left(-29013\cosh\left(2\sqrt{c}\alpha\right) + 2112\cosh\left(4\sqrt{c}\alpha\right) + 13\cosh\left(6\sqrt{c}\alpha\right) + 32248\right)\mathrm{sech}^8\left(\sqrt{c}\alpha\right)}{s^{2\lambda+1}}\\ &+ \frac{c - 2c\mathrm{sech}^2\left(\sqrt{c}\alpha\right)}{s} + \cdots.\end{aligned} \tag{59}$$

$$\begin{aligned}v_2(\alpha,s) &= \frac{c^{7/2}\left(11119\cosh\left(2\sqrt{c}x\right) - 146\cosh\left(4\sqrt{c}x\right) + \cosh\left(6\sqrt{c}x\right) - 14078\right)\mathrm{sech}^7\left(\sqrt{c}x\right)}{4s^{2\lambda+1}}\\ &- \frac{c^2\left(49\sinh\left(\sqrt{c}x\right) + \sinh\left(3\sqrt{c}x\right)\right)\mathrm{sech}^4\left(\sqrt{c}x\right)}{s^{\lambda+1}} + \frac{2\sqrt{c}\,\mathrm{sech}\left(\sqrt{c}x\right)}{s} + \cdots.\end{aligned} \tag{60}$$

Utilising the Aboodh inverse transform results in

$$
\begin{aligned}
v_1(\alpha,\lambda) &= \frac{4c^{5/2}\lambda^p\left(7\cosh\left(2\alpha\sqrt{c}\right)-17\right)\tanh\left(\alpha\sqrt{c}\right)\operatorname{sech}^4\left(\alpha\sqrt{c}\right)}{\Gamma(p+1)} \\
&- \frac{c^4\lambda^{2p}\left(-29013\cosh\left(2\alpha\sqrt{c}\right)+2112\cosh\left(4\alpha\sqrt{c}\right)+13\cosh\left(6\alpha\sqrt{c}\right)+32248\right)\operatorname{sech}^8\left(\alpha\sqrt{c}\right)}{\Gamma(2p+1)} \\
&- 2c\operatorname{sech}^2\left(\alpha\sqrt{c}\right)+c+\cdots.
\end{aligned} \tag{61}
$$

$$
\begin{aligned}
v_2(\alpha,\lambda) &= \frac{c^{7/2}\lambda^{2p}\left(11119\cosh\left(2\alpha\sqrt{c}\right)-146\cosh\left(4\alpha\sqrt{c}\right)+\cosh\left(6\alpha\sqrt{c}\right)-14078\right)\operatorname{sech}^7\left(\alpha\sqrt{c}\right)}{4\Gamma(2p+1)} \\
&- \frac{c^2\lambda^p\left(49\sinh\left(\alpha\sqrt{c}\right)+\sinh\left(3\alpha\sqrt{c}\right)\right)\operatorname{sech}^4\left(\alpha\sqrt{c}\right)}{\Gamma(p+1)}+2\sqrt{c}\operatorname{sech}\left(\alpha\sqrt{c}\right)+16+\cdots.
\end{aligned} \tag{62}
$$

Figure 1 shows the variation in fractional order p for the solution $v_1(\alpha,\lambda)$ for $\lambda = 0.01$ in example 1 using the ARPSM method. The graph depicts the effect of various fractional orders on the solution's behaviour, demonstrating how changes in p affect the solution in relation to the specified parameters. Figure 2 depicts, in both three-dimensional and two-dimensional formats, the effect of varying fractional orders on the $v_1(\alpha,\lambda)$ solution for $\lambda = 0.01$ in example 1. This comparison elucidates the solution's characteristics more vividly, emphasising the importance of fractional order p in determining the solution's behaviour. Table 1 compares different fractional orders used in the ARPSM solution for $v_1(\alpha,\lambda)$ in example 1, with a focus on $\lambda = 0.01$. The table provides a concise summary of the numerical results, allowing for a direct comparison of the solution's performance at different fractional orders. Moving on to Figure 3, which, like Figure 1, shows the variation in the fractional order p of the ARPSM solution for $\lambda = 0.01$, but this time for $v_2(\alpha,\lambda)$ in example 1. The graph shows how p affects the behaviour of the second solution under consideration. Figure 4, like Figure 2, shows a three-dimensional and two-dimensional comparison of the effect of different fractional orders on the $v_2(\alpha,\lambda)$ solution in example 1 for $\lambda = 0.01$. This graphical representation helps to understand how changes in fractional order affect the properties of the solution. Table 2, like Table 1, provides a quantitative summary of the numerical results obtained from the ARPSM solution for $v_2(\alpha,\lambda)$ in example 1, with a focus on $\lambda = 0.01$. These tabulated data are useful for comparing the performance of the solution with different fractional orders.

Table 1. The comparison of different fractional orders of ARPSM solution of example 1 of $v_1(\alpha,\lambda)$ for $\lambda = 0.01$.

α	$ARPSM_{P=0.6}$	$ARPSM_{p=0.8}$	$ARPSM_{P=1.0}$	$Exact$	$Error_{p=0.6}$	$Error_{p=0.8}$	$Error_{p=1.0}$
0	−0.0523823	−0.0501432	−0.0500004	−0.05	0.00238228	0.000143191	4.18800×10^{-7}
0.1	−0.052455	−0.0501279	−0.0499529	−0.0499499	0.00250508	0.00017795	3.01163×10^{-6}
0.2	−0.052399	−0.0500107	−0.0498056	−0.0498001	0.00259898	0.000210666	5.57137×10^{-6}
0.3	−0.0522144	−0.049792	−0.0495591	−0.049551	0.00266333	0.000241	8.07032×10^{-6}
0.4	−0.0519019	−0.0494725	−0.0492143	−0.0492039	0.00269803	0.000268656	1.04818×10^{-5}
0.5	−0.0514634	−0.0490532	−0.0487726	−0.0487599	0.00270358	0.000293385	1.27803×10^{-5}

Table 1. *Cont.*

α	$ARPSM_{P=0.6}$	$ARPSM_{p=0.8}$	$ARPSM_{P=1.0}$	$Exact$	$Error_{p=0.6}$	$Error_{p=0.8}$	$Error_{p=1.0}$
0.6	−0.0509018	−0.0485358	−0.0482357	−0.0482208	0.002681	0.000314992	1.49424×10^{-5}
0.7	−0.0502206	−0.0479221	−0.0476057	−0.0475888	0.00263177	0.000333328	1.69466×10^{-5}
0.8	−0.0494241	−0.0472146	−0.0468851	−0.0468663	0.00255781	0.000348297	1.87738×10^{-5}
0.9	−0.0485174	−0.0464159	−0.0460764	−0.046056	0.0024614	0.000359853	2.04074×10^{-5}
1	−0.0475062	−0.0455291	−0.045183	−0.0451611	0.00234507	0.000367995	2.18338×10^{-5}

Table 2. The comparison of different fractional orders of ARPSM solution of example 1 of $v_2(\alpha, \lambda)$ for $\lambda = 0.01$.

α	$ARPSM_{P=0.6}$	$ARPSM_{p=0.8}$	$ARPSM_{P=1.0}$	$Exact$	$Error_{p=0.6}$	$Error_{p=0.8}$	$Error_{p=1.0}$
0	0.445671	0.447209	0.447213	0.447214	0.00154242	0.000049447	2.71011×10^{-7}
0.1	0.444773	0.447045	0.447087	0.447102	0.00232883	0.0000562121	1.45678×10^{-5}
0.2	0.443671	0.446659	0.446738	0.446766	0.00309533	0.000107159	2.8786×10^{-5}
0.3	0.44237	0.446051	0.446166	0.446209	0.00383819	0.000157518	4.28507×10^{-5}
0.4	0.440876	0.445223	0.445373	0.44543	0.004554	0.000207031	5.66885×10^{-5}
0.5	0.439192	0.444176	0.444362	0.444432	0.00523973	0.000255447	7.02288×10^{-5}
0.6	0.437325	0.442915	0.443134	0.443217	0.00589272	0.000302527	8.34037×10^{-5}
0.7	0.435278	0.441441	0.441693	0.441789	0.00651072	0.000348047	9.61496×10^{-5}
0.8	0.433059	0.439759	0.440042	0.440151	0.00709186	0.000391798	1.08407×10^{-4}
0.9	0.430671	0.437872	0.438186	0.438306	0.00763469	0.000433591	1.20121×10^{-4}
1	0.428121	0.435786	0.436128	0.436259	0.00813811	0.000473254	1.31244×10^{-4}

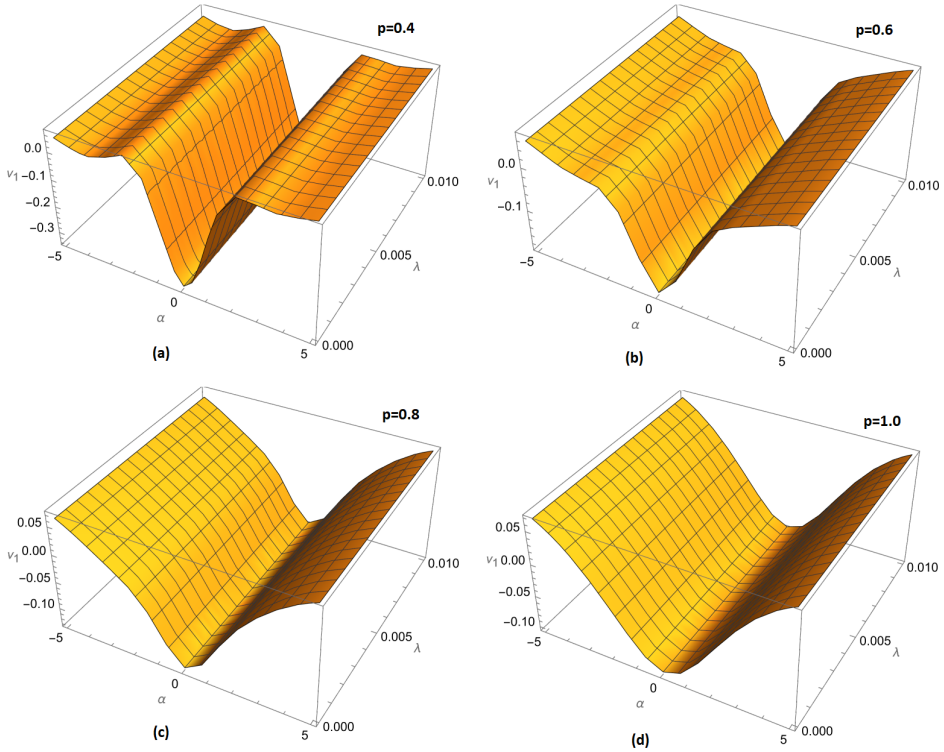

Figure 1. Variation of fractional order (**a**) $p = 0.4$, (**b**) $p = 0.6$, (**c**) $p = 0.8$ and (**d**) $p = 1.0$ for $\lambda = 0.01$ of example 1 ARPSM solution for $v_1(\alpha, \lambda)$.

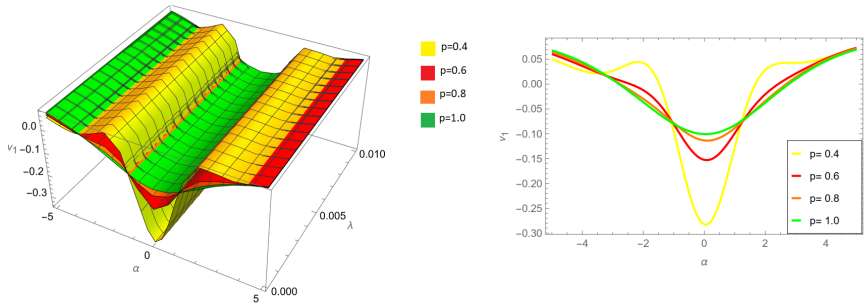

Figure 2. Three-dimensional and two-dimensional comparison of different fractional orders p for $\lambda = 0.01$ of example 1 ARPSM solution for $v_1(\alpha, \lambda)$.

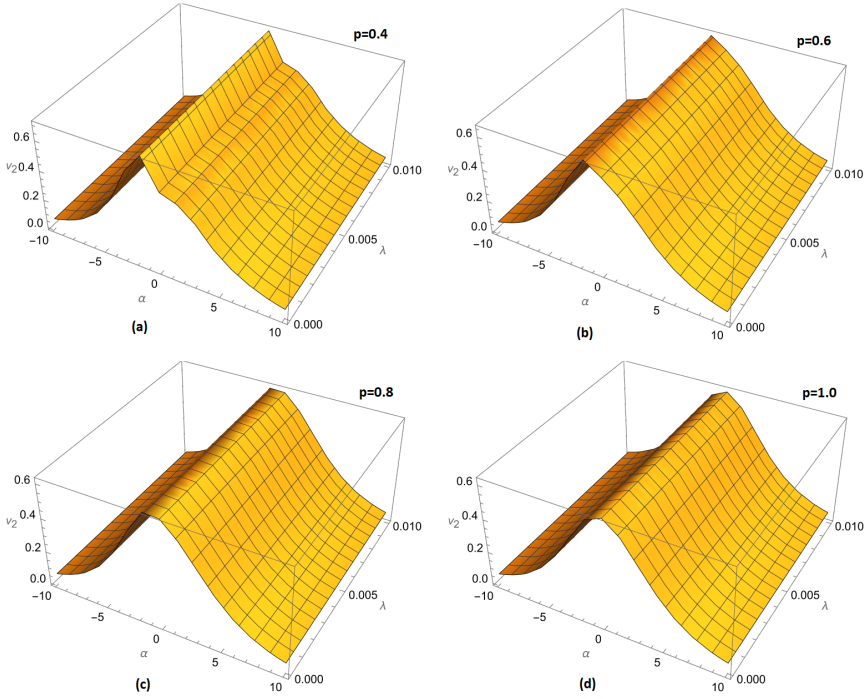

Figure 3. Variation of fractional order (**a**) $p = 0.4$, (**b**) $p = 0.6$, (**c**) $p = 0.8$ and (**d**) $p = 1.0$ for $\lambda = 0.01$ of example 1 ARPSM solution for for $v_2(\alpha, \lambda)$.

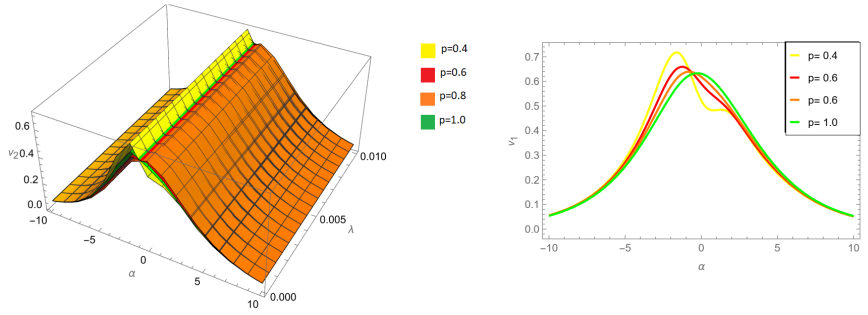

Figure 4. Three-dimensional and two-dimension comparison of different fractional orders p for $\lambda = 0.01$ of example 1 ARPSM solution for $v_2(\alpha, \lambda)$.

3.3. Problem 2

Let us analyze a third-order homogeneous two-component KdV system with a temporal fractional component, presented as follows:

$$D_\lambda^p v_1(\alpha,\lambda) - \frac{\partial^3 v_1(\alpha,\lambda)}{\partial\alpha^3} - v_1(\alpha,\lambda)\frac{\partial v_1(\alpha,\lambda)}{\partial\alpha} - v_2(\alpha,\lambda)\frac{\partial v_2(\alpha,\lambda)}{\partial\alpha} = 0, \tag{63}$$

$$D_\lambda^p v_2(\alpha,\lambda) + 2\frac{\partial^3 v_2(\alpha,\lambda)}{\partial\alpha^3} - v_1(\alpha,\lambda)\frac{\partial v_2(\alpha,\lambda)}{\partial\alpha} = 0, \tag{64}$$

where $0 < p \leq 1$.

With the following IC's:

$$v_1(\alpha,0) = 3 - 6\tanh^2\left(\frac{\alpha}{2}\right), \tag{65}$$

$$v_2(\alpha,0) = -3\sqrt{2}c\tanh\left(\frac{\alpha}{2}\right), \tag{66}$$

and exact solution

$$v_1(\alpha,0) = 3 - 6\tanh^2\left(\frac{\lambda+\alpha}{2}\right), \tag{67}$$

$$v_2(\alpha,0) = -3\sqrt{2}c\tanh\left(\frac{\lambda+\alpha}{2}\right). \tag{68}$$

Equations (65) and (66) are employed, and utilising the Aboodh Transform (AT) on Equations (63) and (64), we obtain:

$$\begin{aligned} &v_1(\alpha,\lambda) - \frac{3-6\tanh^2\left(\frac{\alpha}{2}\right)}{s^2} - \frac{1}{s^p}\mathcal{A}_\lambda\left[\frac{\partial^3\mathcal{A}_\lambda^{-1}v_1(\alpha,\lambda)}{\partial\alpha^3}\right] - \frac{1}{s^p}\mathcal{A}_\lambda\left[\mathcal{A}_\lambda^{-1}v_1(\alpha,\lambda)\frac{\partial\mathcal{A}_\lambda^{-1}v_1(\alpha,\lambda)}{\partial\alpha}\right] \\ &- \mathcal{A}_\lambda\frac{1}{s^p}\left[\mathcal{A}_\lambda^{-1}v_2(\alpha,\lambda)\frac{\partial\mathcal{A}_\lambda^{-1}v_2(\alpha,\lambda)}{\partial\alpha}\right] = 0, \end{aligned} \tag{69}$$

$$v_2(\alpha,\lambda) + \frac{3\sqrt{2}c\tanh\left(\frac{\alpha}{2}\right)}{s^2} + \frac{2}{s^p}\mathcal{A}_\lambda\left[\frac{\partial^3\mathcal{A}_\lambda^{-1}v_2(\alpha,\lambda)}{\partial\alpha^3}\right] - \frac{1}{s^p}\mathcal{A}_\lambda\left[\mathcal{A}_\lambda^{-1}v_1(\alpha,\lambda)\frac{\partial\mathcal{A}_\lambda^{-1}v_2(\alpha,\lambda)}{\partial\alpha}\right] = 0. \tag{70}$$

Hence, the term series that have been k^{th} truncated are

$$v_1(\alpha,s) = \frac{3-6\tanh^2\left(\frac{\alpha}{2}\right)}{s^2} + \sum_{r=1}^{k}\frac{f_r(\alpha,s)}{s^{rp+1}}, \quad r = 1,2,3,4\cdots. \tag{71}$$

$$v_2(\alpha,s) = \frac{-3\sqrt{2}c\tanh\left(\frac{\alpha}{2}\right)}{s^2} + \sum_{r=1}^{k}\frac{g_r(\alpha,s)}{s^{rp+1}}, \quad r = 1,2,3,4\cdots. \tag{72}$$

Aboodh residual functions (ARFs) are

$$\begin{aligned} \mathcal{A}_\lambda Res(\alpha,s) = v_1(\alpha,\lambda) &- \frac{3-6\tanh^2\left(\frac{\alpha}{2}\right)}{s^2} - \frac{1}{s^p}\mathcal{A}_\lambda\left[\frac{\partial^3\mathcal{A}_\lambda^{-1}v_1(\alpha,\lambda)}{\partial\alpha^3}\right] - \frac{1}{s^p}\mathcal{A}_\lambda\left[\mathcal{A}_\lambda^{-1}v_1(\alpha,\lambda)\frac{\partial\mathcal{A}_\lambda^{-1}v_1(\alpha,\lambda)}{\partial\alpha}\right] \\ &- \mathcal{A}_\lambda\frac{1}{s^p}\left[\mathcal{A}_\lambda^{-1}v_2(\alpha,\lambda)\frac{\partial\mathcal{A}_\lambda^{-1}v_2(\alpha,\lambda)}{\partial\alpha}\right] = 0, \end{aligned} \tag{73}$$

$$\begin{aligned} \mathcal{A}_\lambda Res(\alpha,s) = v_2(\alpha,\lambda) &+ \frac{3\sqrt{2}c\tanh\left(\frac{\alpha}{2}\right)}{s^2} + \frac{2}{s^p}\mathcal{A}_\lambda\left[\frac{\partial^3\mathcal{A}_\lambda^{-1}v_2(\alpha,\lambda)}{\partial\alpha^3}\right] \\ &- \frac{1}{s^p}\mathcal{A}_\lambda\left[\mathcal{A}_\lambda^{-1}v_1(\alpha,\lambda)\frac{\partial\mathcal{A}_\lambda^{-1}v_2(\alpha,\lambda)}{\partial\alpha}\right] = 0, \end{aligned} \tag{74}$$

and the k^{th}-LRFs as:

$$\begin{aligned}\mathcal{A}_\lambda Res_k(\alpha,s) &= v_{1,k}(\alpha,\lambda) - \frac{3-6\tanh^2\left(\frac{\alpha}{2}\right)}{s^2} - \frac{1}{s^p}\mathcal{A}_\lambda\left[\frac{\partial^3\mathcal{A}_\lambda^{-1}v_{1,k}(\alpha,\lambda)}{\partial\alpha^3}\right]\\ &- \frac{1}{s^p}\mathcal{A}_\lambda\left[\mathcal{A}_\lambda^{-1}v_{1,k}(\alpha,\lambda)\frac{\partial\mathcal{A}_\lambda^{-1}v_{1,k}(\alpha,\lambda)}{\partial\alpha}\right] - \mathcal{A}_\lambda\frac{1}{s^p}\left[\mathcal{A}_\lambda^{-1}v_{2,k}(\alpha,\lambda)\frac{\partial\mathcal{A}_\lambda^{-1}v_{2,k}(\alpha,\lambda)}{\partial\alpha}\right] = 0,\end{aligned} \tag{75}$$

$$\begin{aligned}\mathcal{A}_\lambda Res_k(\alpha,s) &= v_{2,k}(\alpha,\lambda) + \frac{3\sqrt{2}c\tanh\left(\frac{\alpha}{2}\right)}{s^2} + \frac{2}{s^p}\mathcal{A}_\lambda\left[\frac{\partial^3\mathcal{A}_\lambda^{-1}v_{2,k}(\alpha,\lambda)}{\partial\alpha^3}\right]\\ &- \frac{1}{s^p}\mathcal{A}_\lambda\left[\mathcal{A}_\lambda^{-1}v_{1,k}(\alpha,\lambda)\frac{\partial\mathcal{A}_\lambda^{-1}v_{2,k}(\alpha,\lambda)}{\partial\alpha}\right] = 0.\end{aligned} \tag{76}$$

To compute $f_r(\alpha,s)$ and $g_r(\alpha,s)$, follow these steps: multiply the resulting equations by s^{rp+1}, substitute the r^{th}-truncated series from Equations (71) and (72) into the r^{th}-Aboodh residual function represented by Equations (75) and (76). Then, iteratively solve the relations $\lim_{s\to\infty}(s^{rp+1}A\lambda Resv_1, r(\alpha,s)) = 0$ and $\lim_{s\to\infty}(s^{rp+1}A\lambda Resv_2, r(\alpha,s)) = 0$ for $r = 1,2,3,\cdots$. Here are the first few of terms:

$$\begin{aligned}f_1(\alpha,s) &= \frac{3}{2}\tanh\left(\frac{x}{2}\right)\mathrm{sech}^4\left(\frac{\alpha}{2}\right)\left(\left(3c^2+4\right)\cosh(\alpha)+3c^2-8\right),\\ g_1(\alpha,s) &= \frac{3c(5\cosh(\alpha)-13)\mathrm{sech}^4\left(\frac{\alpha}{2}\right)}{2\sqrt{2}},\end{aligned} \tag{77}$$

$$\begin{aligned}f_2(\alpha,s) &= \frac{3}{32}\mathrm{sech}^8\left(\frac{x}{2}\right)\Big(21c^2\cosh(3\alpha)+\left(99c^2-456\right)\cosh(\alpha)-48\left(6c^2+1\right)\cosh(2\alpha)\\ &+408c^2+8\cosh(3\alpha)+608\Big),\\ g_2(\alpha,s) &= \frac{3c\tanh\left(\frac{\alpha}{2}\right)\mathrm{sech}^6\left(\frac{\alpha}{2}\right)\left(-4\left(9c^2+245\right)\cosh(\alpha)-36c^2+25\cosh(2\alpha)+2163\right)}{8\sqrt{2}},\end{aligned} \tag{78}$$

and so on.

Putting the values of $f_r(\alpha,s)$ and $g_r(\alpha,s)$, $r = 1,2,3,\cdots$, in Equations (71) and (72), we obtain

$$\begin{aligned}v_1(\alpha,s) &= \frac{3-6\tanh^2\left(\frac{\alpha}{2}\right)}{s} + \frac{3\tanh\left(\frac{\alpha}{2}\right)\mathrm{sech}^4\left(\frac{\alpha}{2}\right)\left(\left(3c^2+4\right)\cosh(\alpha)+3c^2-8\right)}{2s^{\lambda+1}}\\ &+\frac{\frac{3}{32}\left(\left(99c^2-456\right)\cosh(\alpha)-48\left(6c^2+1\right)\cosh(2\alpha)+408c^2+608\right.}{s^{2\lambda+1}}\\ &+\frac{\left.21c^2\cosh(3\alpha)+8\cosh(3\alpha)\right)\mathrm{sech}^8\left(\frac{\alpha}{2}\right)}{s^{2\lambda+1}}+\cdots.\end{aligned} \tag{79}$$

$$\begin{aligned}v_2(\alpha,s) &= -\frac{3\sqrt{2}c\tanh\left(\frac{\alpha}{2}\right)}{s} + \frac{3c(5\cosh(\alpha)-13)\mathrm{sech}^4\left(\frac{\alpha}{2}\right)}{\left(2\sqrt{2}\right)s^{\lambda+1}}\\ &+\frac{3c\tanh\left(\frac{\alpha}{2}\right)\mathrm{sech}^6\left(\frac{\alpha}{2}\right)\left(-4\left(9c^2+245\right)\cosh(\alpha)-36c^2+25\cosh(2\alpha)+2163\right)}{\left(8\sqrt{2}\right)s^{2\lambda+1}}+\cdots.\end{aligned} \tag{80}$$

Utilising the Aboodh inverse transform results in

$$v_1(\alpha,\lambda) = \frac{3}{32}\operatorname{sech}^8\left(\frac{\alpha}{2}\right)\Big(-16\cosh^6\left(\frac{\alpha}{2}\right)(\cosh(\alpha)-3) + \frac{\lambda^{2p}\left(\left(99c^2-456\right)\cosh(\alpha)-48\left(6c^2+1\right)\cosh(2\alpha)+\left(21c^2+8\right)\cosh(3\alpha)+8\left(51c^2+76\right)\right)}{\Gamma(2p+1)} + \frac{2\sinh^3(\alpha)\operatorname{csch}^2\left(\frac{\alpha}{2}\right)\lambda^p\left(\left(3c^2+4\right)\cosh(\alpha)+3c^2-8\right)}{\Gamma(p+1)}\Big)+\cdots. \tag{81}$$

$$v_2(\alpha,\lambda) = -\frac{3c\operatorname{sech}^4\left(\frac{\alpha}{2}\right)}{8\sqrt{2}\Gamma(p+1)\Gamma(2p+1)}\Big(\tanh\left(\frac{\alpha}{2}\right)\operatorname{sech}^2\left(\frac{\alpha}{2}\right)\lambda^{2p}\Gamma(p+1)\Big(-121\cosh(2\alpha) + 4\Big(27c^2+893\Big)\cosh(\alpha)+108c^2-7827\Big)+\Gamma(2p+1)\Big(4\sinh(\alpha)(\cosh(\alpha)+1)\Gamma(p+1) - 4(11\cosh(\alpha)-31)\lambda^p\Big)\Big)+\cdots. \tag{82}$$

Figure 5 shows the variation in fractional order p for the solution $v_1(\alpha,\lambda)$ for $\lambda = 0.01$ in example 2 using the ARPSM method. The graph depicts the effect of various fractional orders on the solution's behaviour, demonstrating how changes in p affect the solution in relation to the specified parameters. Figure 6 depicts, in both three-dimensional and two-dimensional formats, the effect of varying fractional orders on the $v_1(\alpha,\lambda)$ solution for $\lambda = 0.01$ in example 2. This comparison elucidates the solution's characteristics more vividly, emphasising the importance of fractional order p in determining the solution's behaviour. Table 3, compares different fractional orders used in the ARPSM solution for $v_1(\alpha,\lambda)$ in example 2, with a focus on $\lambda = 0.01$. The table provides a concise summary of the numerical results, allowing for a direct comparison of the solution's performance at different fractional orders. Moving on to Figure 7, which, like Figure 5, shows the variation in the fractional order p of the ARPSM solution for $\lambda = 0.01$, but this time for $v_2(\alpha,\lambda)$ in example 2. The graph shows how p affects the behaviour of the second solution under consideration. Figure 8, like Figure 6, shows a three-dimensional and two-dimensional comparison of the effect of different fractional orders on the $v_2(\alpha,\lambda)$ solution in example 2 for $\lambda = 0.01$. This graphical representation helps to understand how changes in fractional order affect the properties of the solution. Table 4, like Table 3 provides a quantitative summary of the numerical results obtained from the ARPSM solution for $v_2(\alpha,\lambda)$ in example 1, with a focus on $\lambda = 0.01$. These tabulated data are useful for comparing the performance of the solution with different fractional orders.

Table 3. The comparison of different fractional orders of ARPSM solution of example 2 of $v_1(\alpha,t)$ for $\lambda = 0.01$.

α	$ARPSM_{P=0.6}$	$ARPSM_{p=0.8}$	$ARPSM_{P=1.0}$	*Exact*	$Error_{p=0.7}$	$Error_{p=0.8}$	$Error_{p=1.0}$
−0.5	2.64509	2.64084	2.6402	2.6401	0.00498289	0.000740352	9.74069×10^{-5}
−0.4	2.77074	2.76693	2.76636	2.76627	0.00446789	0.000659444	8.7449×10^{-5}
−0.3	2.87068	2.86755	2.86708	2.86701	0.00367436	0.000536885	7.15344×10^{-5}
−0.2	2.94305	2.94078	2.94045	2.9404	0.00264689	0.000379776	5.06799×10^{-5}
−0.1	2.98648	2.98523	2.98505	2.98503	0.00144809	0.000197893	2.62897×10^{-5}
0.1	2.98387	2.98483	2.985	2.98502	0.00115043	0.00019213	2.61859×10^{-5}
0.2	2.93801	2.94002	2.94034	2.94039	0.00238083	0.000374625	5.05872×10^{-5}
0.3	2.86353	2.86646	2.86692	2.86699	0.00345764	0.000532689	7.14588×10^{-5}
0.4	2.76193	2.76559	2.76616	2.76625	0.00431374	0.00065646	8.73951×10^{-5}
0.5	2.63518	2.63934	2.63998	2.64008	0.00489907	0.000738729	9.73776×10^{-5}

Table 4. The comparison of different fractional orders of ARPSM solution of example 2 of $v_2(\alpha, \lambda)$ for $\lambda = 0.01$.

α	$ARPSM_{P=0.6}$	$ARPSM_{p=0.8}$	$ARPSM_{P=1.0}$	$Exact$	$Error_{p=0.7}$	$Error_{p=0.8}$	$Error_{p=1.0}$
1	−0.199922	−0.196678	−0.196152	−0.196061	0.00386074	0.000617078	9.02631×10^{-5}
1.1	−0.215516	−0.212859	−0.212428	−0.212354	0.0031612	0.000505073	7.36884×10^{-5}
1.2	−0.230353	−0.228251	−0.22791	−0.227852	0.00250073	0.000398811	5.79595×10^{-5}
1.3	−0.244428	−0.24284	−0.242584	−0.24254	0.00188798	0.000299995	4.3334×10^{-5}
1.4	−0.257742	−0.256623	−0.256443	−0.256413	0.00132905	0.000209845	2.9997×10^{-5}
1.5	−0.2703	−0.269601	−0.26949	−0.269472	0.000827636	0.000129125	1.80645×10^{-5}
1.6	−0.282113	−0.281786	−0.281736	−0.281728	0.000385347	0.0000581901	7.590282×10^{-6}
1.7	−0.293199	−0.293194	−0.293196	−0.293197	5.992109×10^{-5}	2.955875×10^{-5}	1.424832×10^{-6}
1.8	−0.303576	−0.303846	−0.303891	−0.3039	0.000324097	5.45956×10^{-5}	9.023568×10^{-6}
1.9	−0.313269	−0.313767	−0.313849	−0.313864	0.000595754	9.72328×10^{-5}	1.5282×10^{-5}
2	−0.322301	−0.322986	−0.323098	−0.323118	0.00081668	0.00013153	2.03×10^{-5}

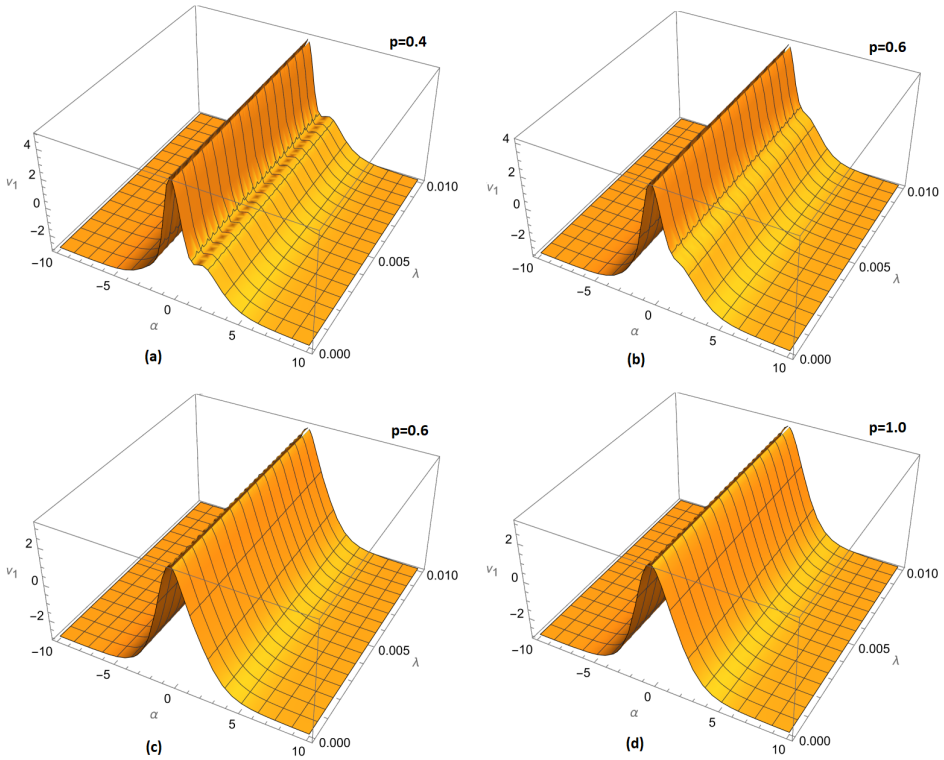

Figure 5. Variation of fractional order (**a**) $p = 0.4$, (**b**) $p = 0.6$, (**c**) $p = 0.8$ and (**d**) $p = 1.0$ for $\lambda = 0.01$ of example 2 ARPSM solution for for $v_1(\alpha, \lambda)$.

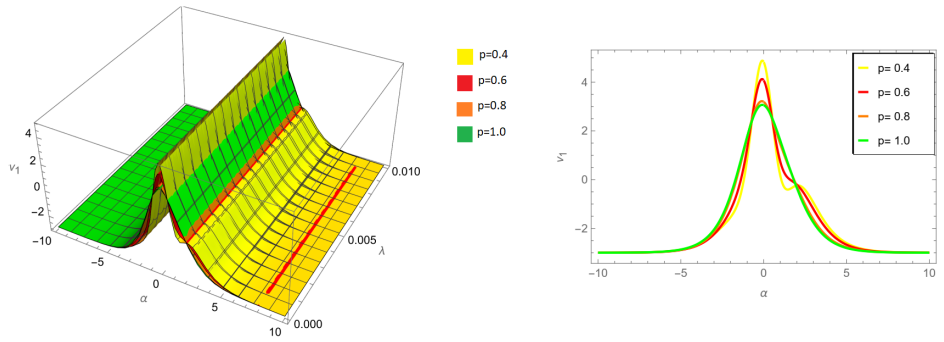

Figure 6. Three-dimensional and two-dimensional comparison of different fractional orders p for $\lambda = 0.01$ of example 2 ARPSM solution for $v_1(\alpha, \lambda)$.

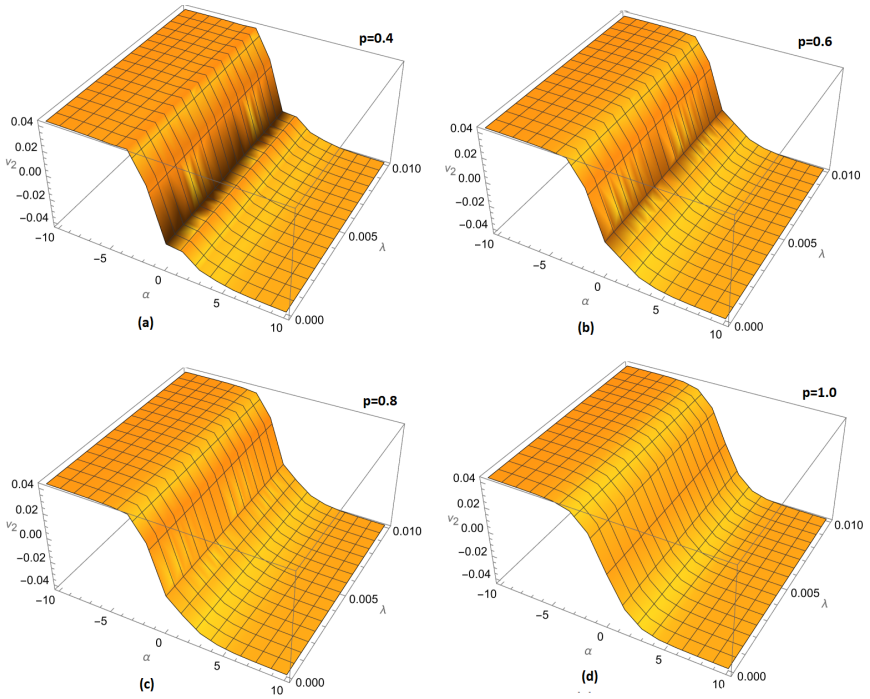

Figure 7. Variation of fractional order (**a**) $p = 0.4$, (**b**) $p = 0.6$, (**c**) $p = 0.8$ and (**d**) $p = 1.0$ for $\lambda = 0.01$ of example 2 ARPSM solution for for $v_2(\alpha, \lambda)$.

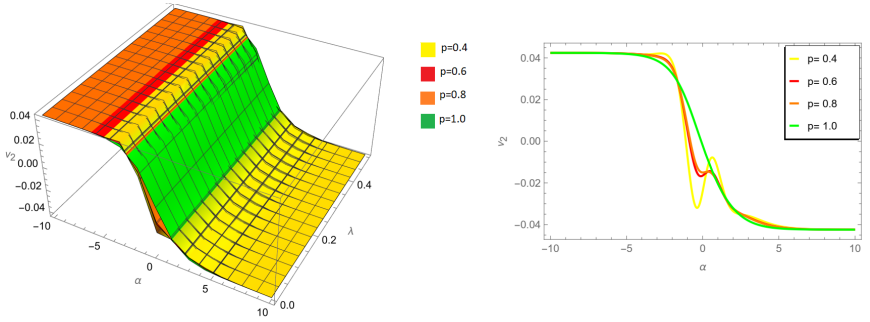

Figure 8. Three-dimensional and two-dimensional comparison of different fractional orders p for $\lambda = 0.01$ of example 2 ARPSM solution for $v_2(\alpha, \lambda)$.

3.4. Fundamental Concept of the Aboodh Transform Iterative Approach

Here, we have the space–time fractional partial differential equation:

$$D_\lambda^p v(\alpha,\lambda) = \Phi\Big(v(\alpha,\lambda), D_\alpha^v v(\alpha,\lambda), D_\alpha^{2v} v(\alpha,\lambda), D_\alpha^{3v} v(\alpha,\lambda)\Big),\ 0 < p, v \le 1, \tag{83}$$

with the initial conditions

$$v^{(k)}(\alpha,0) = h_k,\ k = 0,1,2,\cdots,m-1, \tag{84}$$

where $v(\alpha,\lambda)$ is the unknown function to be determined and $\Phi\Big(v(\alpha,\lambda), D_\alpha^v v(\alpha,\lambda), D_\alpha^{2v} v(\alpha,\lambda), D_\alpha^{3v} v(\alpha,\lambda)\Big)$ can be the linear or nonlinear operator of $v(\alpha,\lambda), D_\alpha^v v(\alpha,\lambda), D_\alpha^{2v} v(\alpha,\lambda)$, and $D_\alpha^{3v} v(\alpha,\lambda)$. For convenience, we represent $v(\alpha,\lambda)$ with v. Therefore, by using the Aboodh transform on both sides of Equation (83), we obtain the following equation:

$$A[v(\alpha,\lambda)] = \frac{1}{s^p}\Big(\sum_{k=0}^{m-1} \frac{v^{(k)}(\alpha,0)}{s^{2-p+k}} + A\Big[\Phi\Big(v(\alpha,\lambda), D_\alpha^v v(\alpha,\lambda), D_\alpha^{2v} v(\alpha,\lambda), D_\alpha^{3v} v(\alpha,\lambda)\Big)\Big]\Big). \tag{85}$$

The resulting equation derived from the inverse Aboodh transformation is:

$$v(\alpha,\lambda) = A^{-1}\Big[\frac{1}{s^p}\Big(\sum_{k=0}^{m-1}\frac{v^{(k)}(\alpha,0)}{s^{2-p+k}} + A\Big[\Phi\Big(v(\alpha,\lambda), D_\alpha^v v(\alpha,\lambda), D_\alpha^{2v} v(\alpha,\lambda), D_\alpha^{3v} v(\alpha,\lambda)\Big)\Big]\Big)\Big]. \tag{86}$$

Iteratively applying the Aboodh transform, a solution is obtained in the form of an infinite series:

$$v(\alpha,\lambda) = \sum_{i=0}^{\infty} v_i. \tag{87}$$

Here, $\Phi\Big(v, D_\alpha^v v, D_\alpha^{2v} v, D_\alpha^{3v} v\Big)$ is a linear or nonlinear operator that can be broken down into the following:

$$\begin{aligned}\Phi\Big(v, D_\alpha^v v, D_\alpha^{2v} v, D_\alpha^{3v} v\Big) &= \Phi\Big(v_0, D_\alpha^v v_0, D_\alpha^{2v} v_0, D_\alpha^{3v} v_0\Big)\\ &+ \sum_{i=0}^{\infty}\Bigg(\Phi\Big(\sum_{k=0}^{i}\Big(v_k, D_\alpha^v v_k, D_\alpha^{2v} v_k, D_\alpha^{3v} v_k\Big)\Big) - \Phi\Big(\sum_{k=1}^{i-1}\Big(v_k, D_\alpha^v v_k, D_\alpha^{2v} v_k, D_\alpha^{3v} v_k\Big)\Big)\Bigg).\end{aligned} \tag{88}$$

Equations (87) and (88) are inserted into Equation (86), resulting in the following equation:

$$\begin{aligned}\sum_{i=0}^{\infty} v_i(\alpha,\lambda) &= A^{-1}\Big[\frac{1}{s^p}\Big(\sum_{k=0}^{m-1}\frac{v^{(k)}(\alpha,0)}{s^{2-p+k}} + A[\Phi(v_0, D_\alpha^v v_0, D_\alpha^{2v} v_0, D_\alpha^{3v} v_0)]\Big)\Big]\\ &+ A^{-1}\Big[\frac{1}{s^p}\Big(A\Big[\sum_{i=0}^{\infty}\Big(\Phi\sum_{k=0}^{i}(v_k, D_\alpha^v v_k, D_\alpha^{2v} v_k, D_\alpha^{3v} v_k)\Big)\Big]\Big)\Big]\\ &- A^{-1}\Big[\frac{1}{s^p}\Big(A\Big[\Big(\Phi\sum_{k=1}^{i-1}(v_k, D_\alpha^v v_k, D_\alpha^{2v} v_k, D_\alpha^{3v} v_k)\Big)\Big]\Big)\Big]\end{aligned} \tag{89}$$

$$\begin{aligned}v_0(\alpha,\lambda) &= A^{-1}\Big[\frac{1}{s^p}\Big(\sum_{k=0}^{m-1}\frac{v^{(k)}(\alpha,0)}{s^{2-p+k}}\Big)\Big],\\ v_1(\alpha,\lambda) &= A^{-1}\Big[\frac{1}{s^p}\Big(A[\Phi(v_0, D_\alpha^v v_0, D_\alpha^{2v} v_0, D_\alpha^{3v} v_0)]\Big)\Big],\\ &\vdots\\ v_{m+1}(\alpha,\lambda) &= A^{-1}\Big[\frac{1}{s^p}\Big(A\Big[\sum_{i=0}^{\infty}\Big(\Phi\sum_{k=0}^{i}(v_k, D_\alpha^v v_k, D_\alpha^{2v} v_k, D_\alpha^{3v} v_k)\Big)\Big]\Big)\Big]\\ &- A^{-1}\Big[\frac{1}{s^p}\Big(A\Big[\Big(\Phi\sum_{k=1}^{i-1}(v_k, D_\alpha^v v_k, D_\alpha^{2v} v_k, D_\alpha^{3v} v_k)\Big)\Big]\Big)\Big],\ m = 1, 2, \cdots.\end{aligned} \tag{90}$$

The analytically derived approximate solution for the m-term obtained from Equation (83) is expressed as:

$$v(\alpha,\lambda) = \sum_{i=0}^{m-1} v_i. \tag{91}$$

3.4.1. Problem with NITM

3.4.2. Problem 1

$$\begin{aligned}D_\lambda^p v_1(\alpha,\lambda) &= -\frac{\partial^3 v_1(\alpha,\lambda)}{\partial\alpha^3} + 6v_1(\alpha,\lambda)\frac{\partial v_1(\alpha,\lambda)}{\partial\alpha} - 3v_2(\alpha,\lambda)\frac{\partial^3 v_2(\alpha,\lambda)}{\partial\alpha^3} - 3\frac{\partial}{\partial\alpha}v_2(\alpha,\lambda)\frac{\partial^2}{\partial\alpha^2}v_2(\alpha,\lambda)\\ &+ 3v_2^2(\alpha,\lambda)\frac{\partial v_1(\alpha,\lambda)}{\partial\alpha} - 6v_1(\alpha,\lambda)v_2(\alpha,\lambda)\frac{\partial v_2(\alpha,\lambda)}{\partial\alpha},\end{aligned} \tag{92}$$

$$D_\lambda^p v_2(\alpha,\lambda) = -\frac{\partial^3 v_2(\alpha,\lambda)}{\partial\alpha^3} + 3v_2^2(\alpha,\lambda)\frac{\partial v_2(\alpha,\lambda)}{\partial\alpha} + 3v_1(\alpha,\lambda)\frac{\partial v_2(\alpha,\lambda)}{\partial\alpha} - 3v_2(\alpha,\lambda)\frac{\partial v_1(\alpha,\lambda)}{\partial\alpha}, \quad \text{where} \quad 0 < p \leq 1 \tag{93}$$

With the following IC's:

$$v_1(\alpha,0) = c - 2c\,\operatorname{sech}^2\big(\sqrt{c}\alpha\big), \tag{94}$$

$$v_2(\alpha,0) = 2\sqrt{c}\operatorname{sech}\big(\sqrt{c}\alpha\big). \tag{95}$$

The following equations arise when both sides of Equations (92) and (93) are subjected to the Aboodh transform:

$$A[D_\lambda^p v_1(\alpha,\lambda)] = \frac{1}{s^p}\Big(\sum_{k=0}^{m-1}\frac{v_1^{(k)}(\alpha,0)}{s^{2-p+k}} + A\Big[-\frac{\partial^3 v_1(\alpha,\lambda)}{\partial\alpha^3} + 6v_1(\alpha,\lambda)\frac{\partial v_1(\alpha,\lambda)}{\partial\alpha} - 3v_2(\alpha,\lambda)\frac{\partial^3 v_2(\alpha,\lambda)}{\partial\alpha^3} - 3\frac{\partial}{\partial\alpha}v_2(\alpha,\lambda)\frac{\partial^2}{\partial\alpha^2}v_2(\alpha,\lambda) + 3v_2^2(\alpha,\lambda)\frac{\partial v_1(\alpha,\lambda)}{\partial\alpha} - 6v_1(\alpha,\lambda)v_2(\alpha,\lambda)\frac{\partial v_2(\alpha,\lambda)}{\partial\alpha}\Big]\Big) \tag{96}$$

$$A[D_\lambda^p v_2(\alpha,\lambda)] = \frac{1}{s^p}\Big(\sum_{k=0}^{m-1}\frac{v_2^{(k)}(\alpha,0)}{s^{2-p+k}} + A\Big[-\frac{\partial^3 v_2(\alpha,\lambda)}{\partial\alpha^3} + 3v_2^2(\alpha,\lambda)\frac{\partial v_2(\alpha,\lambda)}{\partial\alpha} + 3v_1(\alpha,\lambda)\frac{\partial v_2(\alpha,\lambda)}{\partial\alpha} - 3v_2(\alpha,\lambda)\frac{\partial v_1(\alpha,\lambda)}{\partial\alpha}\Big]\Big) \tag{97}$$

Applying the inverse Aboodh transform to Equations (96) and (97) yields the following equations:

$$v_1(\alpha,\lambda) = A^{-1}\Big[\frac{1}{s^p}\Big(\sum_{k=0}^{m-1}\frac{v_1^{(k)}(\alpha,0)}{s^{2-p+k}} + A\Big[-\frac{\partial^3 v_1(\alpha,\lambda)}{\partial\alpha^3} + 6v_1(\alpha,\lambda)\frac{\partial v_1(\alpha,\lambda)}{\partial\alpha} - 3v_2(\alpha,\lambda)\frac{\partial^3 v_2(\alpha,\lambda)}{\partial\alpha^3} - 3\frac{\partial}{\partial\alpha}v_2(\alpha,\lambda)\frac{\partial^2}{\partial\alpha^2}v_2(\alpha,\lambda) + 3v_2^2(\alpha,\lambda)\frac{\partial v_1(\alpha,\lambda)}{\partial\alpha} - 6v_1(\alpha,\lambda)v_2(\alpha,\lambda)\frac{\partial v_2(\alpha,\lambda)}{\partial\alpha}\Big]\Big)\Big] \tag{98}$$

$$v_2(\alpha,\lambda) = A^{-1}\Big[\frac{1}{s^p}\Big(\sum_{k=0}^{m-1}\frac{v_2^{(k)}(\alpha,0)}{s^{2-p+k}} + A\Big[-\frac{\partial^3 v_2(\alpha,\lambda)}{\partial\alpha^3} + 3v_2^2(\alpha,\lambda)\frac{\partial v_2(\alpha,\lambda)}{\partial\alpha} + 3v_1(\alpha,\lambda)\frac{\partial v_2(\alpha,\lambda)}{\partial\alpha} - 3v_2(\alpha,\lambda)\frac{\partial v_1(\alpha,\lambda)}{\partial\alpha}\Big]\Big)\Big] \tag{99}$$

The subsequent equation is derived through an iterative application of the Aboodh transform:

$$\begin{aligned}(v_1)_0(\alpha,\lambda) &= A^{-1}\Big[\frac{1}{s^p}\Big(\sum_{k=0}^{m-1}\frac{v_1^{(k)}(\alpha,0)}{s^{2-p+k}}\Big)\Big]\\ &= A^{-1}\Big[\frac{v_1(\alpha,0)}{s^2}\Big]\\ &= c - 2c\,\operatorname{sech}^2\big(\sqrt{c}\alpha\big),\end{aligned}$$

$$\begin{aligned}(v_2)_0(\alpha,\lambda) &= A^{-1}\Big[\frac{1}{s^p}\Big(\sum_{k=0}^{m-1}\frac{v_2^{(k)}(\alpha,0)}{s^{2-p+k}}\Big)\Big]\\ &= A^{-1}\Big[\frac{v_2(\alpha,0)}{s^2}\Big]\\ &= 2\sqrt{c}\operatorname{sech}\big(\sqrt{c}\alpha\big).\end{aligned}$$

We obtain the equivalent form by applying the R–L integral to Equations (92) and (93).

$$v_1(\alpha,\lambda) = c - 2c\,\mathrm{sech}^2\left(\sqrt{c}\alpha\right) + A\Big[-\frac{\partial^3 v_1(\alpha,\lambda)}{\partial\alpha^3} + 6v_1(\alpha,\lambda)\frac{\partial v_1(\alpha,\lambda)}{\partial\alpha} - 3v_2(\alpha,\lambda)\frac{\partial^3 v_2(\alpha,\lambda)}{\partial\alpha^3} - 3\frac{\partial}{\partial\alpha}v_2(\alpha,\lambda)\frac{\partial^2}{\partial\alpha^2}v_2(\alpha,\lambda) + 3v_2^2(\alpha,\lambda)\frac{\partial v_1(\alpha,\lambda)}{\partial\alpha} - 6v_1(\alpha,\lambda)v_2(\alpha,\lambda)\frac{\partial v_2(\alpha,\lambda)}{\partial\alpha}\Big] \tag{100}$$

$$v_2(\alpha,t) = 2\sqrt{c}\mathrm{sech}\left(\sqrt{c}\alpha\right) + A\Big[-\frac{\partial^3 v_2(\alpha,\lambda)}{\partial\alpha^3} + 3v_2^2(\alpha,\lambda)\frac{\partial v_2(\alpha,\lambda)}{\partial\alpha} + 3v_1(\alpha,\lambda)\frac{\partial v_2(\alpha,\lambda)}{\partial\alpha} - 3v_2(\alpha,\lambda)\frac{\partial v_1(\alpha,\lambda)}{\partial\alpha}\Big] \tag{101}$$

The NITM process yields the following few terms:

$$\begin{aligned} v_{10}(\alpha,\lambda) &= c - 2c\,\mathrm{sech}^2\left(\sqrt{c}\alpha\right),\\ v_{20}(\alpha,\lambda) &= 2\sqrt{c}\mathrm{sech}\left(\sqrt{c}\alpha\right),\\ v_{11}(\alpha,\lambda) &= \frac{4c^{5/2}\lambda^p\left(7\cosh\left(2\alpha\sqrt{c}\right)-17\right)\tanh\left(\alpha\sqrt{c}\right)\mathrm{sech}^4\left(\alpha\sqrt{c}\right)}{\Gamma(p+1)},\\ v_{21}(\alpha,\lambda) &= -\frac{2c^2\lambda^p\left(\cosh\left(2\alpha\sqrt{c}\right)+25\right)\tanh\left(\alpha\sqrt{c}\right)\mathrm{sech}^3\left(\alpha\sqrt{c}\right)}{\Gamma(p+1)}, \end{aligned} \tag{102}$$

$$\begin{aligned} &v_{12}(\alpha,\lambda) = \frac{1}{2}c^4\lambda^{2p}\mathrm{sech}^8\left(\alpha\sqrt{c}\right)\\ &\Big(-\frac{2\Big(-29013\cosh\left(2\alpha\sqrt{c}\right)+2112\cosh\left(4\alpha\sqrt{c}\right)+13\cosh\left(6\alpha\sqrt{c}\right)+32248\Big)}{\Gamma(2p+1)}\\ &+3c^{3/2}\lambda^p\tanh\left(\alpha\sqrt{c}\right)\mathrm{sech}^2\left(\alpha\sqrt{c}\right)\times\\ &\Big(8c^{3/2}\lambda^p\Gamma(3p+1)^2\Big(-69777\cosh\left(2\alpha\sqrt{c}\right)+16182\cosh\left(4\alpha\sqrt{c}\right)+353\cosh\left(6\alpha\sqrt{c}\right)+80282\Big)\tanh\left(\alpha\sqrt{c}\right)\\ &\mathrm{sech}^2\left(\alpha\sqrt{c}\right)\div\Gamma(4p+1)+\Gamma(p+1)\Gamma(2p+1)\Big(-514776\cosh\left(2\alpha\sqrt{c}\right)\\ &+36668\cosh\left(4\alpha\sqrt{c}\right)-232\cosh\left(6\alpha\sqrt{c}\right)+\cosh\left(8\alpha\sqrt{c}\right)+609539\Big)\Big)\div\Gamma(p+1)^3\Gamma(3p+1)\Big). \end{aligned} \tag{103}$$

$$\begin{aligned} &v_{22}(\alpha,\lambda) = \frac{1}{4}c^{7/2}\lambda^{2p}\mathrm{sech}^7\left(\alpha\sqrt{c}\right)\Big(-8c^{3/2}\lambda^p\Gamma(2p+1)\left(6507\cosh\left(2\alpha\sqrt{c}\right)+6\cosh\left(4\alpha\sqrt{c}\right)+5\cosh\left(6\alpha\sqrt{c}\right)-11926\right)\\ &\tanh\left(\alpha\sqrt{c}\right)\mathrm{sech}^2\left(\alpha\sqrt{c}\right)\div p\Gamma(3p)\Gamma(p+1)^2\\ &+\frac{24c^3\lambda^{2p}\Gamma(3p+1)\left(\cosh\left(2\alpha\sqrt{c}\right)+25\right)^2\left(140\cosh\left(2\alpha\sqrt{c}\right)+\cosh\left(4\alpha\sqrt{c}\right)-245\right)\tanh^2\left(\alpha\sqrt{c}\right)\mathrm{sech}^4\left(\alpha\sqrt{c}\right)}{\Gamma(p+1)^3\Gamma(4p+1)}\\ &+\frac{11119\cosh\left(2\alpha\sqrt{c}\right)-146\cosh\left(4\alpha\sqrt{c}\right)+\cosh\left(6\alpha\sqrt{c}\right)-14078}{\Gamma(2p+1)}\Big). \end{aligned}$$

The ultimate result of the NITM algorithm is under

$$v_1(\alpha,\lambda) = v_{10}(\alpha,\lambda) + v_{11}(\alpha,\lambda) + v_{12}(\alpha,\lambda) + \cdots. \tag{104}$$

$$v_2(\alpha,\lambda) = v_{20}(\alpha,\lambda) + v_{21}(\alpha,\lambda) + v_{22}(\alpha,\lambda) + \cdots. \tag{105}$$

$$
\begin{aligned}
v_1(\alpha,\lambda) = {} & \frac{4c^{5/2}\lambda^p\left(7\cosh\left(2\alpha\sqrt{c}\right)-17\right)\tanh\left(\alpha\sqrt{c}\right)\operatorname{sech}^4\left(\alpha\sqrt{c}\right)}{\Gamma(p+1)} + \frac{1}{2}c^4\lambda^{2p}\operatorname{sech}^8\left(\alpha\sqrt{c}\right)\Bigg(3c^{3/2}\lambda^p\tanh\left(\alpha\sqrt{c}\right) \\
& \operatorname{sech}^2\left(\alpha\sqrt{c}\right)\Bigg(8c^{3/2}\lambda^p\Gamma(3p+1)^2\left(-69777\cosh\left(2\alpha\sqrt{c}\right)+16182\cosh\left(4\alpha\sqrt{c}\right)+353\cosh\left(6\alpha\sqrt{c}\right)+80282\right)\tanh\left(\alpha\sqrt{c}\right) \\
& \operatorname{sech}^2\left(\alpha\sqrt{c}\right) \div \Gamma(4p+1) + \Gamma(p+1)\Gamma(2p+1)\Bigg(-514776\cosh\left(2\alpha\sqrt{c}\right)+36668\cosh\left(4\alpha\sqrt{c}\right)-232\cosh\left(6\alpha\sqrt{c}\right) \\
& +\cosh\left(8\alpha\sqrt{c}\right)+609539\Bigg)\Bigg) \div \Gamma(p+1)^3\Gamma(3p+1) \\
& -\frac{2\left(-29013\cosh\left(2\alpha\sqrt{c}\right)+2112\cosh\left(4\alpha\sqrt{c}\right)+13\cosh\left(6\alpha\sqrt{c}\right)+32248\right)}{\Gamma(2p+1)}\Bigg) - 2c\operatorname{sech}^2\left(\alpha\sqrt{c}\right)+c+\cdots.
\end{aligned}
\tag{106}
$$

$$
\begin{aligned}
v_2(\alpha,\lambda) = {} & -\frac{2c^2\lambda^p\left(\cosh\left(2\alpha\sqrt{c}\right)+25\right)\tanh\left(\alpha\sqrt{c}\right)\operatorname{sech}^3\left(\alpha\sqrt{c}\right)}{\Gamma(p+1)} + \frac{1}{4}c^{7/2}\lambda^{2p}\operatorname{sech}^7\left(\alpha\sqrt{c}\right) \\
& \Bigg(-\frac{8c^{3/2}\lambda^p\Gamma(2p+1)\left(6507\cosh\left(2\alpha\sqrt{c}\right)+6\cosh\left(4\alpha\sqrt{c}\right)+5\cosh\left(6\alpha\sqrt{c}\right)-11926\right)\tanh\left(\alpha\sqrt{c}\right)\operatorname{sech}^2\left(\alpha\sqrt{c}\right)}{p\Gamma(3p)\Gamma(p+1)^2} \\
& +\frac{24c^3\lambda^{2p}\Gamma(3p+1)\left(\cosh\left(2\alpha\sqrt{c}\right)+25\right)^2\left(140\cosh\left(2\alpha\sqrt{c}\right)+\cosh\left(4\alpha\sqrt{c}\right)-245\right)\tanh^2\left(\alpha\sqrt{c}\right)\operatorname{sech}^4\left(\alpha\sqrt{c}\right)}{\Gamma(p+1)^3\Gamma(4p+1)} \\
& +\frac{11119\cosh\left(2\alpha\sqrt{c}\right)-146\cosh\left(4\alpha\sqrt{c}\right)+\cosh\left(6\alpha\sqrt{c}\right)-14078}{\Gamma(2p+1)}\Bigg) + 2\sqrt{c}\operatorname{sech}\left(\alpha\sqrt{c}\right)+\cdots.
\end{aligned}
\tag{107}
$$

Figure 9 shows the variation in fractional order p for the solution $v_1(\alpha,\lambda)$ for $\lambda = 0.01$ in example 1 using the NIT method. The graph depicts the effect of various fractional orders on the solution's behaviour, demonstrating how changes in p affect the solution in relation to the specified parameters. Figure 10 depicts, in both three-dimensional and two-dimensional formats, the effect of varying fractional orders on the $v_1(\alpha,\lambda)$ solution for $\lambda = 0.01$ in example 1. This comparison elucidates the solution's characteristics more vividly, emphasising the importance of fractional order p in determining the solution's behaviour. Table 5 compares different fractional orders used in the NITM solution for $v_1(\alpha,\lambda)$ in example 1, with a focus on $\lambda = 0.01$. The table provides a concise summary of the numerical results, allowing for a direct comparison of the solution's performance at different fractional orders. Moving on to Figure 11, which, like Figure 9, shows the variation in the fractional order p of the NITM solution for $\lambda = 0.01$, but this time for $v_2(\alpha,\lambda)$ in example 1. The graph shows how p affects the behaviour of the second solution under consideration. Figure 12, like Figure 10, shows a three-dimensional and two-dimensional comparison of the effect of different fractional orders on the $v_2(\alpha,\lambda)$ solution in example 1 for $\lambda = 0.01$. This graphical representation helps to understand how changes in fractional order affect the properties of the solution. Table 6, like Table 5, provides a quantitative summary of the numerical results obtained from the NITM solution for $v_2(\alpha,\lambda)$ in example 1, with a focus on $\lambda = 0.01$. These tabulated data are useful for comparing the performance of the solution with different fractional orders.

Table 5. The comparison of different fractional orders of NITM solution of example 1 of $v_1(\alpha,\lambda)$ for $\lambda = 0.01$.

α	$NITM_{P=0.6}$	$NITM_{p=0.8}$	$NITM_{P=1.0}$	$Exact$	$Error_{p=0.6}$	$Error_{p=0.8}$	$Error_{p=1.0}$
0	−0.0591648	−0.0500335	−0.05	−0.05	0.00916479	0.0000335001	1.680000×10^{-8}
0.1	−0.059281	−0.0500011	−0.0499505	−0.0499499	0.00933107	0.0000512042	6.157033×10^{-7}
0.2	−0.0591906	−0.0498684	−0.0498013	−0.0498001	0.00939052	0.0000683243	1.208437×10^{-6}

Table 5. *Cont.*

α	$NITM_{P=0.6}$	$NITM_{p=0.8}$	$NITM_{P=1.0}$	$Exact$	$Error_{p=0.6}$	$Error_{p=0.8}$	$Error_{p=1.0}$
0.3	−0.0588959	−0.0496357	−0.0495528	−0.049551	0.00934484	0.0000846762	1.789121×10^{-6}
0.4	−0.0584016	−0.0493039	−0.0492062	−0.0492039	0.00919779	0.00010009	2.352063×10^{-6}
0.5	−0.0577148	−0.0488743	−0.0487627	−0.0487599	0.00895499	0.00011441	2.891837×10^{-6}
0.6	−0.0568445	−0.0483483	−0.0482242	−0.0482208	0.0086237	0.000127501	3.403370×10^{-6}
0.7	−0.0558014	−0.047728	−0.0475927	−0.0475888	0.00821261	0.000139246	3.882007×10^{-6}
0.8	−0.0545978	−0.0470158	−0.0468706	−0.0468663	0.00773151	0.000149549	4.323579×10^{-6}
0.9	−0.0532471	−0.0462144	−0.0460608	−0.046056	0.00719103	0.000158334	4.724447×10^{-6}
1	−0.0517634	−0.0453267	−0.0451662	−0.0451611	0.00660231	0.000165549	5.081553×10^{-6}

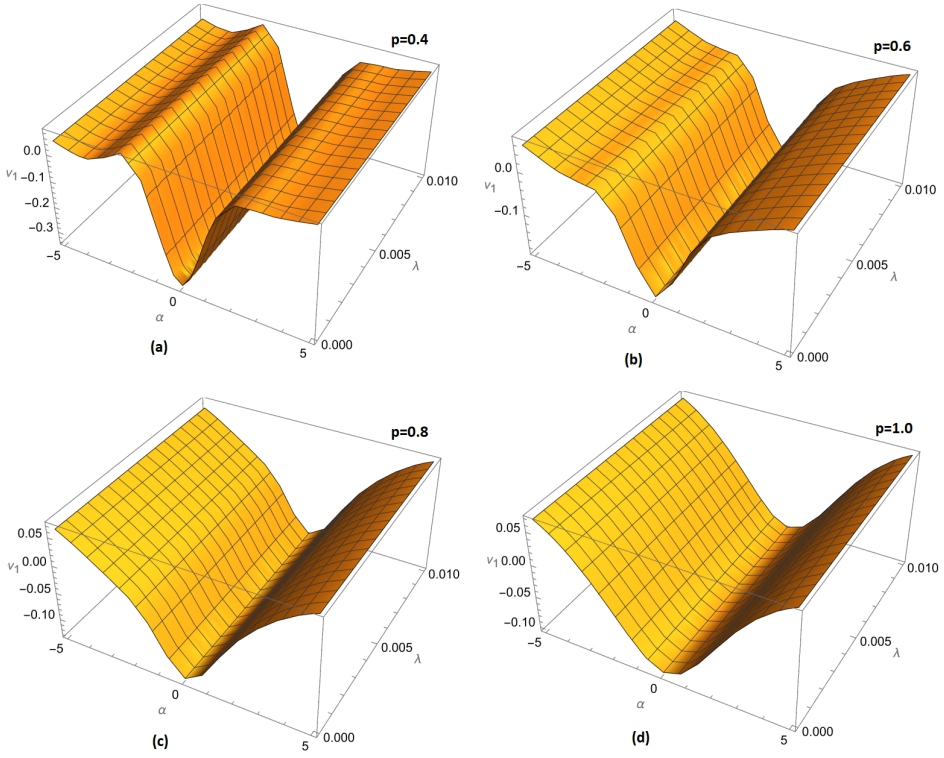

Figure 9. Variation of fractional order (**a**) $p = 0.4$, (**b**) $p = 0.6$, (**c**) $p = 0.8$ and (**d**) $p = 1.0$ for $\lambda = 0.01$ of example 1 NITM solution for $v_1(\alpha, \lambda)$.

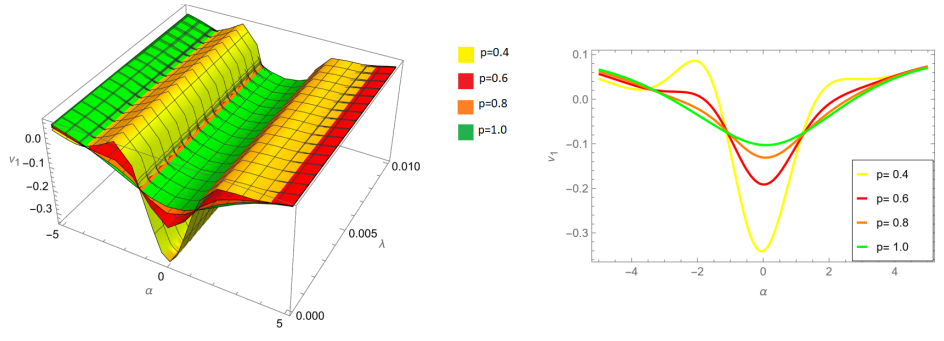

Figure 10. Three-dimensional and two-dimensional comparison of different fractional order p for $\lambda = 0.01$ of example 1 NITM solution for $v_1(\alpha, \lambda)$.

Table 6. The comparison of different fractional orders of NITM solution of example 1 of $v_2(\alpha, \lambda)$ for $\lambda = 0.01$.

α	$NITM_{P=0.6}$	$NITM_{p=0.8}$	$NITM_{P=1.0}$	$Exact$	$Error_{p=0.6}$	$Error_{p=0.8}$	$Error_{p=1.0}$
0	0.44128	0.447192	0.447214	0.447214	0.00593382	0.0000216897	3.354094×10^{-12}
0.1	0.439701	0.446977	0.447102	0.447102	0.00740105	0.000124982	6.691626×10^{-8}
0.2	0.437966	0.446539	0.446766	0.446766	0.00880056	0.000227508	1.328656×10^{-7}
0.3	0.436082	0.44588	0.446208	0.446209	0.0101265	0.000328737	1.968883×10^{-7}
0.4	0.434055	0.445002	0.44543	0.44543	0.0113743	0.000428148	2.580538×10^{-7}
0.5	0.431892	0.443907	0.444432	0.444432	0.0125402	0.000525246	3.154696×10^{-7}
0.6	0.429596	0.442598	0.443217	0.443217	0.0136218	0.000619558	3.682926×10^{-7}
0.7	0.427172	0.441078	0.441789	0.441789	0.0146174	0.000710642	4.157401×10^{-7}
0.8	0.424624	0.439353	0.44015	0.440151	0.0155266	0.000798088	4.570989×10^{-7}
0.9	0.421956	0.437424	0.438305	0.438306	0.0163496	0.000881527	4.917337×10^{-7}
1	0.419172	0.435299	0.436259	0.436259	0.0170875	0.000960626	5.190937×10^{-7}

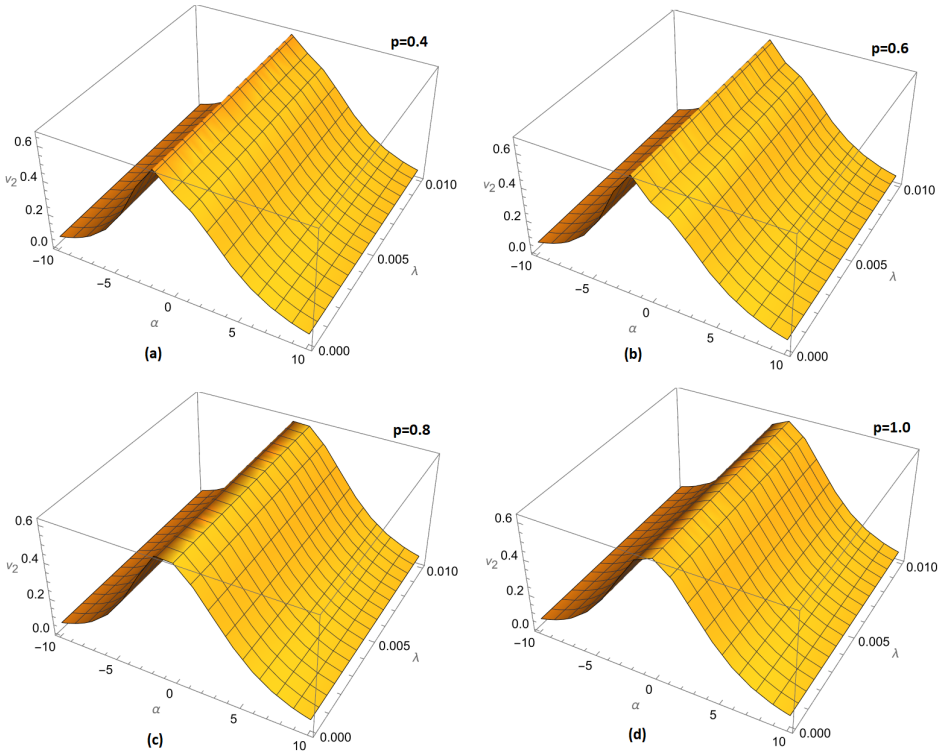

Figure 11. Variation of fractional order (**a**) $p = 0.4$, (**b**) $p = 0.6$, (**c**) $p = 0.8$ and (**d**) $p = 1.0$ for $\lambda = 0.01$ of example 1 NITM solution for $v_2(\alpha, \lambda)$.

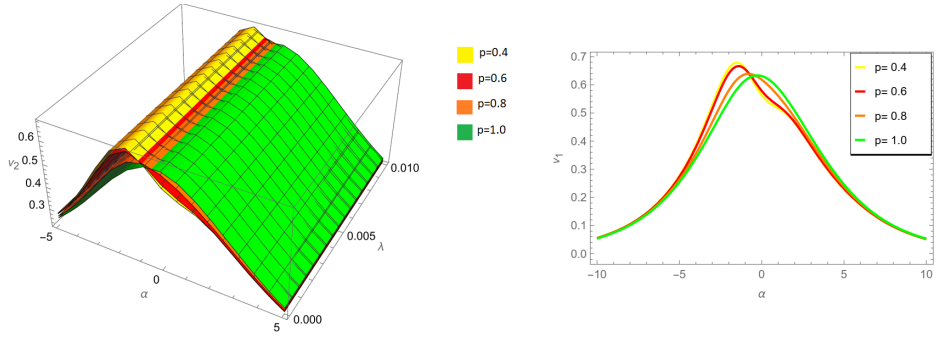

Figure 12. Three-dimensional and two-dimensional comparison of different fractional order p for $\lambda = 0.01$ of example 1 NITM solution for $v_2(\alpha, \lambda)$.

3.4.3. Problem 2

$$D_\lambda^p v_1(\alpha,\lambda) = \frac{\partial^3 v_1(\alpha,\lambda)}{\partial\alpha^3} + v_1(\alpha,\lambda)\frac{\partial v_1(\alpha,\lambda)}{\partial\alpha} + v_2(\alpha,\lambda)\frac{\partial v_2(\alpha,\lambda)}{\partial\alpha}, \tag{108}$$

$$D_\lambda^p v_2(\alpha,\lambda) = -2\frac{\partial^3 v_2(\alpha,\lambda)}{\partial\alpha^3} + v_1(\alpha,\lambda)\frac{\partial v_2(\alpha,\lambda)}{\partial\alpha}, \text{ where } 0 < p \le 1. \tag{109}$$

With the IC's:

$$v_1(\alpha,0) = 3 - 6\tanh^2\Big(\frac{\alpha}{2}\Big), \tag{110}$$

$$v_2(\alpha,0) = -3\sqrt{2}c\tanh\Big(\frac{\alpha}{2}\Big). \tag{111}$$

The following equations arise when both sides of Equations (108) and (109) are subjected to the Aboodh transform:

$$A[D_\lambda^p v_1(\alpha,\lambda)] = \frac{1}{s^p}\Big(\sum_{k=0}^{m-1}\frac{v_1^{(k)}(\alpha,0)}{s^{2-p+k}} + A\Big[\frac{\partial^3 v_1(\alpha,\lambda)}{\partial\alpha^3} + v_1(\alpha,\lambda)\frac{\partial v_1(\alpha,\lambda)}{\partial\alpha} + v_2(\alpha,\lambda)\frac{\partial v_2(\alpha,\lambda)}{\partial\alpha}\Big]\Big), \tag{112}$$

$$A[D_\lambda^p v_2(\alpha,\lambda)] = \frac{1}{s^p}\Big(\sum_{k=0}^{m-1}\frac{v_2^{(k)}(\alpha,0)}{s^{2-p+k}} + A\Big[-2\frac{\partial^3 v_2(\alpha,\lambda)}{\partial\alpha^3} + v_1(\alpha,\lambda)\frac{\partial v_2(\alpha,\lambda)}{\partial\alpha}\Big]\Big). \tag{113}$$

The following equations are obtained by applying the inverse Aboodh transform to Equations (112) and (113):

$$v_1(\alpha,\lambda) = A^{-1}\Big[\frac{1}{s^p}\Big(\sum_{k=0}^{m-1}\frac{v_1^{(k)}(\alpha,0)}{s^{2-p+k}} + A\Big[\frac{\partial^3 v_1(\alpha,\lambda)}{\partial\alpha^3} + v_1(\alpha,\lambda)\frac{\partial v_1(\alpha,\lambda)}{\partial\alpha} + v_2(\alpha,\lambda)\frac{\partial v_2(\alpha,\lambda)}{\partial\alpha}\Big]\Big)\Big], \tag{114}$$

$$v_2(\alpha,\lambda) = A^{-1}\Big[\frac{1}{s^p}\Big(\sum_{k=0}^{m-1}\frac{v_2^{(k)}(\alpha,0)}{s^{2-p+k}} + A\Big[-2\frac{\partial^3 v_2(\alpha,\lambda)}{\partial\alpha^3} + v_1(\alpha,\lambda)\frac{\partial v_2(\alpha,\lambda)}{\partial\alpha}\Big]\Big)\Big]. \tag{115}$$

The subsequent equation is derived through an iterative application of the Aboodh transform:

$$\begin{aligned}(v_1)_0(\alpha,\lambda) &= A^{-1}\Big[\frac{1}{s^p}\Big(\sum_{k=0}^{m-1}\frac{v_1^{(k)}(\alpha,0)}{s^{2-p+k}}\Big)\Big]\\ &= A^{-1}\Big[\frac{v_1(\alpha,0)}{s^2}\Big]\\ &= 3 - 6\tanh^2\Big(\frac{\alpha}{2}\Big),\end{aligned}$$

$$\begin{aligned}(v_2)_0(\alpha,\lambda) &= A^{-1}\Big[\frac{1}{s^p}\Big(\sum_{k=0}^{m-1}\frac{v_2^{(k)}(\alpha,0)}{s^{2-p+k}}\Big)\Big]\\ &= A^{-1}\Big[\frac{v_2(\alpha,0)}{s^2}\Big]\\ &= -3\sqrt{2}c\tanh\Big(\frac{\alpha}{2}\Big),\end{aligned}$$

By applying R–L integral to Equations (108) and (109), we obtain the equivalent form:

$$v_1(\alpha,\lambda) = 3 - 6\tanh^2\Big(\frac{\alpha}{2}\Big) + A\Big[\frac{\partial^3 v_1(\alpha,\lambda)}{\partial\alpha^3} + v_1(\alpha,\lambda)\frac{\partial v_1(\alpha,\lambda)}{\partial\alpha} + v_2(\alpha,\lambda)\frac{\partial v_2(\alpha,\lambda)}{\partial\alpha}\Big], \tag{116}$$

$$v_2(\alpha,\lambda) = -3\sqrt{2}c\tanh\Big(\frac{\alpha}{2}\Big) + A\Big[-2\frac{\partial^3 v_2(\alpha,\lambda)}{\partial\alpha^3} + v_1(\alpha,\lambda)\frac{\partial v_2(\alpha,\lambda)}{\partial\alpha}\Big]. \tag{117}$$

According to the NITM procedure, we obtain the following few terms:

$$\begin{aligned} v_{10}(\alpha,\lambda) &= 3-6\tanh^2\Big(\frac{\alpha}{2}\Big),\\ v_{20}(\alpha,\lambda) &= -3\sqrt{2}c\tanh\Big(\frac{\alpha}{2}\Big),\\ v_{11}(\alpha,\lambda) &= \frac{3\tanh\big(\frac{\alpha}{2}\big)\mathrm{sech}^4\big(\frac{\alpha}{2}\big)\lambda^p\big(\big(3c^2+4\big)\cosh(\alpha)+3c^2-8\big)}{2\Gamma(p+1)},\\ v_{21}(\alpha,\lambda) &= \frac{3c(5\cosh(\alpha)-13)\mathrm{sech}^4\big(\frac{\alpha}{2}\big)\lambda^p}{2\sqrt{2}\Gamma(p+1)}, \end{aligned} \tag{118}$$

$$\begin{aligned} v_{12}(\alpha,\lambda) &= 3\lambda^{2p}\mathrm{sech}^8\Big(\frac{\alpha}{2}\Big)\Big(6\Big(33c^2-152\Big)\cosh(\alpha)-96\Big(6c^2+1\Big)\cosh(2\alpha)+2\Big(21c^2+8\Big)\cosh(3\alpha)+16\Big(51c^2+76\Big)\\ &-\Big(3\lambda^p\Gamma(2p+1)^2\tanh\Big(\frac{\alpha}{2}\Big)\mathrm{sech}^2\Big(\frac{\alpha}{2}\Big)\Big(-6\Big(137c^2+96\Big)\cosh(2\alpha)+\Big(2c^2+1\Big)\Big(9c^2+32\Big)\cosh(3\alpha)\\ &+3\Big(-54c^4+317c^2+928\Big)\cosh(\alpha)-2\Big(72c^4-923c^2+1184\Big)\Big)\Big)\div\Gamma(p+1)^2\Gamma(3p+1)\Big)\div 64\Gamma(2p+1)\\ v_{22}(\alpha,\lambda) &= 3c\lambda^{2p}\tanh\Big(\frac{\alpha}{2}\Big)\mathrm{sech}^6\Big(\frac{\alpha}{2}\Big)\Big(\frac{-4\Big(9c^2+245\Big)\cosh(\alpha)-36c^2+25\cosh(2\alpha)+2163}{8\sqrt{2}\Gamma(2p+1)}\\ &-\frac{3\,2^{2p+1}\lambda^p\Gamma\Big(p+\frac{1}{2}\Big)(5\cosh(\alpha)-31)\tanh\Big(\frac{\alpha}{2}\Big)\mathrm{sech}^2\Big(\frac{\alpha}{2}\Big)\Big(\Big(3c^2+4\Big)\cosh(\alpha)+3c^2-8\Big)}{8\sqrt{2\pi}\Gamma(p+1)\Gamma(3p+1)}\Big). \end{aligned} \tag{119}$$

The ultimate result of the NITM algorithm is under

$$v_1(\alpha,\lambda) = v_{10}(\alpha,\lambda)+v_{11}(\alpha,\lambda)+v_{12}(\alpha,\lambda)+\cdots, \tag{120}$$

$$v_2(\alpha,\lambda) = v_{20}(\alpha,\lambda)+v_{21}(\alpha,\lambda)+v_{22}(\alpha,\lambda)+\cdots. \tag{121}$$

$$\begin{aligned} v(\alpha,t) &= 3-6\tanh^2\Big(\frac{\alpha}{2}\Big)+\frac{3\tanh\big(\frac{\alpha}{2}\big)\mathrm{sech}^4\big(\frac{\alpha}{2}\big)\lambda^p\big(\big(3c^2+4\big)\cosh(\alpha)+3c^2-8\big)}{2\Gamma(p+1)}\\ &+\Big(3\lambda^{2p}\mathrm{sech}^8\Big(\frac{\alpha}{2}\Big)\Big(6\Big(33c^2-152\Big)\cosh(\alpha)-96\Big(6c^2+1\Big)\cosh(2\alpha)+2\Big(21c^2+8\Big)\cosh(3\alpha)+16\Big(51c^2+76\Big)\\ &-\Big(3\lambda^p\Gamma(2p+1)^2\tanh\Big(\frac{\alpha}{2}\Big)\mathrm{sech}^2\Big(\frac{\alpha}{2}\Big)\Big(-6\Big(137c^2+96\Big)\cosh(2\alpha)+\Big(2c^2+1\Big)\Big(9c^2+32\Big)\cosh(3\alpha)\\ &+3\Big(-54c^4+317c^2+928\Big)\cosh(\alpha)-2\Big(72c^4-923c^2+1184\Big)\Big)\Big)\Gamma(p+1)^2\Gamma(3p+1)\Big)\Big)\div 64\Gamma(2p+1)+\cdots. \end{aligned} \tag{122}$$

$$\begin{aligned} w(\alpha,t) &= -3\sqrt{2}c\tanh\Big(\frac{\alpha}{2}\Big)+\frac{3c(5\cosh(\alpha)-13)\mathrm{sech}^4\big(\frac{\alpha}{2}\big)\lambda^p}{2\sqrt{2}\Gamma(p+1)}\\ &+3c\lambda^{2p}\tanh\Big(\frac{\alpha}{2}\Big)\mathrm{sech}^6\Big(\frac{\alpha}{2}\Big)\Big(\frac{-4\Big(9c^2+245\Big)\cosh(\alpha)-36c^2+25\cosh(2\alpha)+2163}{8\sqrt{2}\Gamma(2p+1)}\\ &-\frac{3\,2^{2p+1}\lambda^p\Gamma\Big(p+\frac{1}{2}\Big)(5\cosh(\alpha)-31)\tanh\Big(\frac{\alpha}{2}\Big)\mathrm{sech}^2\Big(\frac{\alpha}{2}\Big)\Big(\Big(3c^2+4\Big)\cosh(\alpha)+3c^2-8\Big)}{8\sqrt{2\pi}\Gamma(p+1)\Gamma(3p+1)}\Big)+\cdots. \end{aligned} \tag{123}$$

Figure 13 shows the variation in fractional order p for the solution $v_1(\alpha,\lambda)$ for $\lambda = 0.01$ in example 2 using the NITM. The graph depicts the effect of various fractional orders on the solution's behaviour, demonstrating how changes in p affect the solution in relation to the specified parameters. Figure 14 depicts, in both three-dimensional and two-dimensional

formats, the effect of varying fractional orders on the $v_1(\alpha, \lambda)$ solution for $\lambda = 0.01$ in example 2. This comparison elucidates the solution's characteristics more vividly, emphasising the importance of fractional order p in determining the solution's behaviour. Table 7 compares different fractional orders used in the NITM solution for $v_1(\alpha, \lambda)$ in example 2, with a focus on $\lambda = 0.01$. The table provides a concise summary of the numerical results, allowing for a direct comparison of the solution's performance at different fractional orders. Moving on to Figure 15, which, like Figure 13, shows the variation in the fractional order p of the NITM solution for $\lambda = 0.01$, but this time for $v_2(\alpha, \lambda)$ in example 2. The graph shows how p affects the behaviour of the second solution under consideration. Figure 16, like Figure 14, shows a three-dimensional and two-dimensional comparison of the effect of different fractional orders on the $v_2(\alpha, \lambda)$ solution in example 2 for $\lambda = 0.01$. This graphical representation helps to understand how changes in fractional order affect the properties of the solution. Table 8, like Table 7, provides a quantitative summary of the numerical results obtained from the NITM solution for $v_2(\alpha, \lambda)$ in example 2, with a focus on $\lambda = 0.01$. These tabulated data are useful for comparing the performance of the solution with different fractional orders. Tables 9 and 10 show a comparison of absolute error for $\lambda = 0.01$ of ARPSM and NITM solution of example 1 for $v_1(\alpha, \lambda)$ and $w_2(\alpha, \lambda)$. Similarly, Tables 11 and 12 present a comparison of absolute error for $\lambda = 0.01$ of ARPSM and NITM solution of example 2 for $v_1(\alpha, \lambda)$ and $w_2(\alpha, \lambda)$.

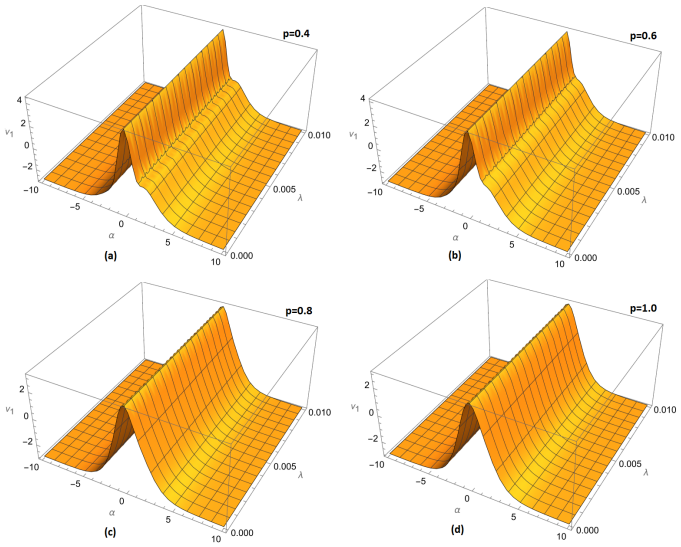

Figure 13. Variation of fractional order (**a**) $p = 0.4$, (**b**) $p = 0.6$, (**c**) $p = 0.8$ and (**d**) $p = 1.0$ for $\lambda = 0.01$ of example 2 NITM solution for $v_1(\alpha, \lambda)$.

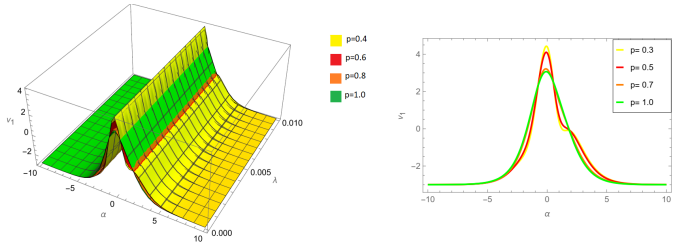

Figure 14. Three-dimensional and two-dimensional comparison of different fractional order p for $\lambda = 0.01$ of example 2 NITM solution for $v_1(\alpha, \lambda)$.

Table 7. The comparison of different fractional orders of NITM solution of example 2 of $v_1(\alpha, \lambda)$ for $\lambda = 0.01$.

α	$NITM_{P=0.6}$	$NITM_{p=0.8}$	$NITM_{P=1.0}$	$Exact$	$Error_{p=0.6}$	$Error_{p=0.8}$	$Error_{p=1.0}$
-0.5	2.64134	2.64021	2.6401	2.6401	0.00123342	0.000105605	2.692781×10^{-6}
-0.4	2.76737	2.76636	2.76627	2.76627	0.00109926	0.0000947386	1.500451×10^{-6}
-0.3	2.8679	2.86709	2.86701	2.86701	0.000896034	0.0000774602	7.113980×10^{-7}
-0.2	2.94104	2.94046	2.9404	2.9404	0.000635413	0.0000548648	2.646464×10^{-7}
-0.1	2.98536	2.98506	2.98503	2.98503	0.000333511	0.0000284636	6.657231×10^{-8}
0.1	2.98471	2.98499	2.98502	2.98502	0.000314729	0.0000283185	6.790399×10^{-8}
0.2	2.93977	2.94034	2.94039	2.94039	0.000618625	0.0000547351	2.658594×10^{-7}
0.3	2.86611	2.86691	2.86699	2.86699	0.00088236	0.0000773546	7.124251×10^{-7}
0.4	2.76516	2.76615	2.76625	2.76625	0.00108954	0.0000946634	1.501242×10^{-6}
0.5	2.63885	2.63997	2.64008	2.64008	0.00122813	0.000105564	2.693303×10^{-6}

Table 8. The comparison of different fractional orders of NITM solution of example 2 of $v_2(\alpha, \lambda)$ for $\lambda = 0.01$.

α	$NITM_{P=0.6}$	$NITM_{p=0.8}$	$NITM_{P=1.0}$	$Exact$	$Error_{p=0.6}$	$Error_{p=0.8}$	$Error_{p=1.0}$
1	-0.197541	-0.196293	-0.196063	-0.196061	0.00147921	0.000231952	1.798267×10^{-6}
1.1	-0.213538	-0.21254	-0.212356	-0.212354	0.00118324	0.000185393	1.184791×10^{-6}
1.2	-0.228756	-0.227994	-0.227853	-0.227852	0.000904042	0.00014133	6.100023×10^{-7}
1.3	-0.243186	-0.242641	-0.242541	-0.24254	0.000645635	0.000100483	8.379734×10^{-8}
1.4	-0.256824	-0.256476	-0.256412	-0.256413	0.000410844	0.000063362	3.869535×10^{-7}
1.5	-0.269674	-0.269502	-0.269471	-0.269472	0.000201381	0.000030285	7.982325×10^{-7}
1.6	-0.281746	-0.28173	-0.281727	-0.281728	0.000017965	0.000013933	1.148569×10^{-6}
1.7	-0.293058	-0.293174	-0.293196	-0.293197	0.000139526	0.000023324	1.438657×10^{-6}
1.8	-0.303629	-0.303856	-0.303899	-0.3039	0.000271908	0.000043998	1.670929×10^{-6}
1.9	-0.313484	-0.313803	-0.313862	-0.313864	0.000380528	0.000060854	1.849134×10^{-6}
2	-0.322651	-0.323044	-0.323116	-0.323118	0.000467126	0.000074184	1.977937×10^{-6}

Table 9. The comparison of absolute error for $\lambda = 0.01$ of ARPSM and NITM solution of example 1 for $v_1(\alpha, \lambda)$.

α	Exact	$ARPSM_P = 1$	$NITM_P = 1$	ARPSM Error	NITM Error
0	-0.05	-0.0500004	-0.05	4.187999×10^{-7}	1.680000×10^{-8}
0.1	-0.0499499	-0.0499529	-0.0499505	3.01163×10^{-6}	6.157033×10^{-7}
0.2	-0.0498001	-0.0498056	-0.0498013	5.57137×10^{-6}	1.208437×10^{-6}
0.3	-0.049551	-0.0495591	-0.0495528	8.07032×10^{-6}	1.789121×10^{-6}
0.4	-0.0492039	-0.0492143	-0.0492062	1.04818×10^{-5}	2.352063×10^{-6}
0.5	-0.0487599	-0.0487726	-0.0487627	1.27803×10^{-5}	2.891837×10^{-6}
0.6	-0.0482208	-0.0482357	-0.0482242	1.49424×10^{-5}	3.403370×10^{-6}
0.7	-0.0475888	-0.0476057	-0.0475927	1.69466×10^{-5}	3.882007×10^{-6}
0.8	-0.0468663	-0.0468851	-0.0468706	1.87738×10^{-5}	4.323579×10^{-6}
0.9	-0.046056	-0.0460764	-0.0460608	2.04074×10^{-5}	4.724447×10^{-6}
1	-0.0451611	-0.045183	-0.0451662	2.18338×10^{-5}	5.081553×10^{-6}

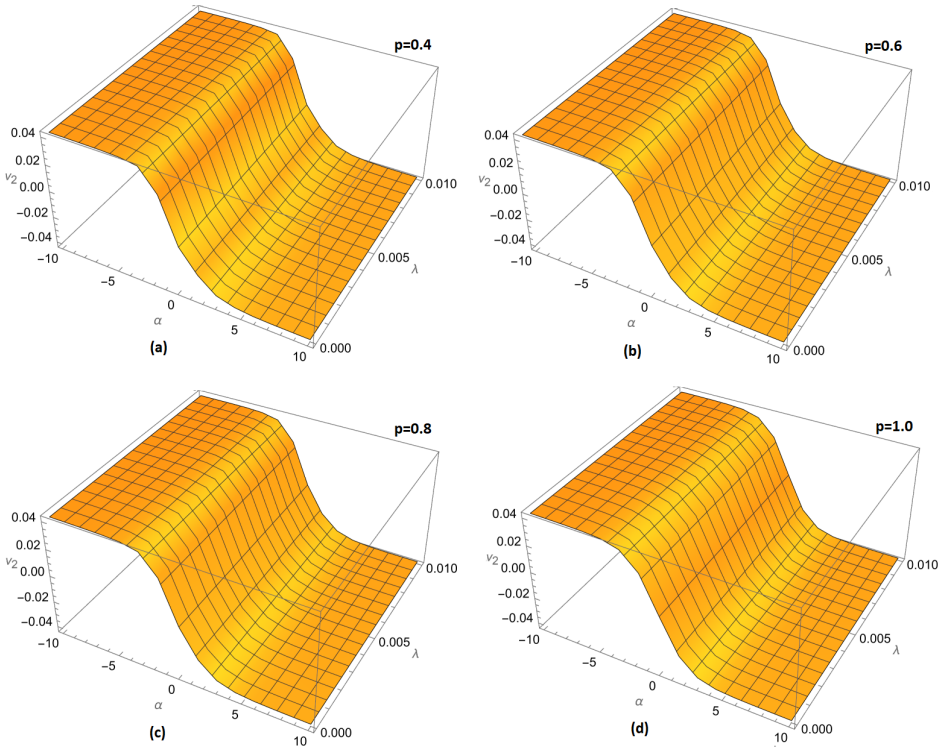

Figure 15. Variation of fractional order (**a**) $p = 0.4$, (**b**) $p = 0.6$, (**c**) $p = 0.8$ and (**d**) $p = 1.0$ for $\lambda = 0.01$ of example 2 NITM solution for $v_2(\alpha, \lambda)$.

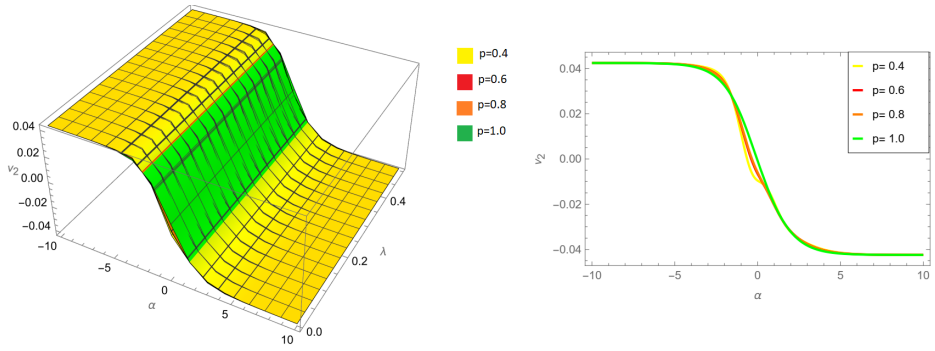

Figure 16. Three-dimensional and two-dimensional comparison of different fractional order p for $\lambda = 0.01$ of example 2 NITM solution for $v_2(\alpha, \lambda)$.

Table 10. The comparison of absolute error for $\lambda = 0.01$ of ARPSM and NITM solution of example 1 for $w_2(\alpha, \lambda)$.

α	Exact	$ARPSM_P = 1$	$NITM_P = 1$	ARPSM Error	NITM Error
0	0.447214	0.447213	0.447214	2.71011×10^{-7}	3.35410×10^{-12}
0.1	0.447102	0.447087	0.447102	1.45678×10^{-5}	6.69162×10^{-8}
0.2	0.446766	0.446738	0.446766	2.8786×10^{-5}	1.32865×10^{-7}
0.3	0.446209	0.446166	0.446208	4.28507×10^{-5}	1.96888×10^{-7}
0.4	0.44543	0.445373	0.44543	5.66885×10^{-5}	2.58053×10^{-7}
0.5	0.444432	0.444362	0.444432	7.02288×10^{-5}	3.15469×10^{-7}
0.6	0.443217	0.443134	0.443217	8.34037×10^{-5}	3.68292×10^{-7}
0.7	0.441789	0.441693	0.441789	9.61496×10^{-5}	4.15740×10^{-7}
0.8	0.440151	0.440042	0.44015	1.08407×10^{-4}	4.57098×10^{-7}
0.9	0.438306	0.438186	0.438305	1.20121×10^{-4}	4.91733×10^{-7}
1	0.436259	0.436128	0.436259	1.31244×10^{-4}	5.19093×10^{-7}

Table 11. The comparison of absolute error for $\lambda = 0.01$ of ARPSM and NITM solution of example 2 for $v_1(\alpha, \lambda)$.

α	Exact	$ARPSM_P = 1$	$NITM_P = 1$	ARPSM Error	NITM Error
-0.5	2.6401	2.6402	2.6401	9.74069×10^{-5}	2.692781×10^{-6}
-0.4	2.76627	2.76636	2.76627	8.7449×10^{-5}	1.500451×10^{-6}
-0.3	2.86701	2.86708	2.86701	7.15344×10^{-5}	7.113980×10^{-7}
-0.2	2.9404	2.94045	2.9404	5.06799×10^{-5}	2.646464×10^{-7}
-0.1	2.98503	2.98505	2.98503	2.62897×10^{-5}	6.657231×10^{-8}
0.1	2.98502	2.985	2.98502	2.61859×10^{-5}	6.790399×10^{-8}
0.2	2.94039	2.94034	2.94039	5.05872×10^{-5}	2.658594×10^{-7}
0.3	2.86699	2.86692	2.86699	7.14588×10^{-5}	7.124251×10^{-7}
0.4	2.76625	2.76616	2.76625	8.73951×10^{-5}	1.501242×10^{-6}
0.5	2.64008	2.63998	2.64008	9.73776×10^{-5}	2.693303×10^{-6}

Table 12. The comparison of absolute error for $\lambda = 0.01$ of ARPSM and NITM solution of example 2 for $v_2(\alpha, \lambda)$.

α	Exact	$ARPSM_P = 1$	$NITM_P = 1$	ARPSM Error	NITM Error
1	-0.196061	-0.196152	-0.196063	9.02631×10^{-5}	1.79826×10^{-6}
1.1	-0.212354	-0.212428	-0.212356	7.36884×10^{-5}	1.18479×10^{-6}
1.2	-0.227852	-0.22791	-0.227853	5.79595×10^{-5}	6.10002×10^{-7}
1.3	-0.24254	-0.242584	-0.242541	4.3334×10^{-5}	8.37973×10^{-8}
1.4	-0.256413	-0.256443	-0.256412	2.9997×10^{-5}	3.86953×10^{-7}
1.5	-0.269472	-0.26949	-0.269471	1.80645×10^{-5}	7.98232×10^{-7}
1.6	-0.281728	-0.281736	-0.281727	7.59028×10^{-6}	1.14856×10^{-6}
1.7	-0.293197	-0.293196	-0.293196	1.42483×10^{-6}	1.43865×10^{-6}
1.8	-0.3039	-0.303891	-0.303899	9.02356×10^{-6}	1.67092×10^{-6}
1.9	-0.313864	-0.313849	-0.313862	1.5282×10^{-5}	1.84913×10^{-6}
2	-0.323118	-0.323098	-0.323116	2.03×10^{-5}	1.97793×10^{-6}

4. Conclusions

In conclusion, the application of the new transform iteration method (NTIM) and the residual power series transform method (RPSTM) in solving fractional nonlinear Korteweg–de Vries (FNKdV) equations has been demonstrated effectively in this study. The computational analyses and results presented through tables and figures showcase the efficiency, accuracy, and computational feasibility of these innovative methods in obtaining solutions for FNKdV equations involving fractional derivatives. The comparative analysis against existing methods highlights the superiority of NTIM and RPSTM, emphasising their potential for addressing complex nonlinear equations with fractional derivatives. The success of these methods not only contributes to advancing the understanding of FNKdV equations, but also suggests a broader applicability in solving similar challenging mathematical models efficiently and accurately. This research underscores the promising prospects of NTIM and RPSTM as powerful tools in the field of nonlinear mathematical modelling involving fractional derivatives. The successful application of the NTIM and the RPSTM in solving FNKdV equations provides a robust foundation for future research endeavors. Further investigations can explore the extension of these innovative methods to tackle a broader spectrum of complex nonlinear equations involving fractional derivatives, elucidating their efficacy and reliability across diverse mathematical models.

Author Contributions: Conceptualization, M.M.A.-S.; Methodology, Z.A.; Software, Y.J.; Validation, Z.A.; Formal analysis, M.M.A.-S.; Investigation, Y.J.; Resources, Z.A. and M.M.A.-S.; Writing—review & editing, Y.J. All authors have read and agreed to the published version of the manuscript.

Funding: This research has been funded by Deputy for Research & Innovation, Ministry of Education through Initiative of Institutional Funding at University of Ha'il Saudi Arabia through project number IFP-22 242.

Data Availability Statement: Data sharing is not applicable to this article as no new data were created or analyzed in this study.

Acknowledgments: This research has been funded by Deputy for Research & Innovation, Ministry of Education through Initiative of Institutional Funding at University of Ha'il Saudi Arabia through project number IFP-22 242.

Conflicts of Interest: The authors declare no conflict of interest.

Nomenclature

α	Spatial coordinate
λ	Temporal coordinate
p	Order factor of the fractional operator
D_{λ}^{p}	Caputo fractional derivative operator
$v_1(\alpha, \lambda)$	Function representing a component of the fractional coupled system
$v_2(\alpha, \lambda)$	Function representing another component of the fractional coupled system
KdV	Korteweg–de Vries equation
mKdV	Modified Korteweg–de Vries equation
ARPSM	Aboodh residual power series method
NTIM	New transform iterative technique
RPSM	Residual power series method
DE	Differential equations
FODEs	Fractional-order differential equations
NITM	Aboodh transform iterative technique
PDEs	Partial differential equations

References

1. Sierociuk, D.; Skovranek, T.; Macias, M.; Podlubny, I.; Petras, I.; Dzielinski, A.; Ziubinski, P. Diffusion process modeling by using fractional-order models. *Appl. Math. Comput.* **2015**, *257*, 2–11. [CrossRef]
2. Arora, S.; Mebrek-Oudina, F.; Sahani, S. Super convergence analysis of fully discrete Hermite splines to simulate wave behaviour of Kuramoto-Sivashinsky equation. *Wave Motion* **2023**, *121*, 103187.
3. Sabatier, J.; Lanusse, P.; Melchior, P.; Oustaloup, A.; Sabatier, J.; Farges, C.; Oustaloup, A. Fractional order models. In *Fractional Order Differentiation and Robust Control Design: CRONE, H-Infinity and Motion Control*; Springer: Berlin/Heidelberg, Germany, 2015; pp. 1–61.
4. Saad Alshehry, A.; Imran, M.; Khan, A.; Weera, W. Fractional View Analysis of Kuramoto-Sivashinsky Equations with Non-Singular Kernel Operators. *Symmetry* **2022**, *14*, 1463. [CrossRef]
5. Tepljakov, A.; Tepljakov, A. FOMCON: Fractional-order modeling and control toolbox. In *Fractional-Order Modeling and Control of Dynamic Systems*; Springer: Berlin/Heidelberg, Germany, 2017; pp. 107–129.
6. Botmart, T.; Agarwal, R.P.; Naeem, M.; Khan, A. On the solution of fractional modified Boussinesq and approximate long wave equations with non-singular kernel operators. *AIMS Math.* **2022**, *7*, 12483–12513. [CrossRef]
7. Bagley, R.L.; Calico, R.A. Fractional order state equations for the control of viscoelasticallydamped structures. *J. Guid. Control. Dyn.* **1991**, *14*, 304–311. [CrossRef]
8. Podlubny, I. *Fractional-Order Systems and Fractional-Order Controllers*; Institute of Experimental Physics, Slovak Academy of Sciences: Kosice, Slovakia, 1994; Volume 12, pp. 1–18.
9. Yasmin, H.; Aljahdaly, N.H.; Saeed, A.M. Probing families of optical soliton solutions in fractional perturbed Radhakrishnan-Kundu-Lakshmanan model with improved versions of extended direct algebraic method. *Fractal Fract.* **2023**, *7*, 512. [CrossRef]
10. Yasmin, H.; Aljahdaly, N.H.; Saeed, A.M. Investigating Families of Soliton Solutions for the Complex Structured Coupled Fractional Biswas-Arshed Model in Birefringent Fibers Using a Novel Analytical Technique. *Fractal Fract.* **2023**, *7*, 491. [CrossRef]
11. Naeem, M.; Zidan, A.M.; Nonlaopon, K.; Syam, M.I.; Al-Zhour, Z.; Shah, R. A new analysis of fractional-order equal-width equations via novel techniques. *Symmetry* **2021**, *13*, 886. [CrossRef]
12. Iqbal, N.; Akgul, A.; Shah, R.; Bariq, A.; Mossa Al-Sawalha, M.; Ali, A. On solutions of fractional-order gas dynamics equation by effective techniques. *J. Funct. Spaces* **2022**, *2022*, 3341754. [CrossRef]
13. Sunthrayuth, P.; Zidan, A.M.; Yao, S.W.; Shah, R.; Inc, M. The comparative study for solving fractional-order Fornberg-Whitham equation via ρ-Laplace transform. *Symmetry* **2021**, *13*, 784. [CrossRef]
14. Alesemi, M.; Iqbal, N.; Botmart, T. Novel analysis of the fractional-order system of non-linear partial differential equations with the exponential-decay kernel. *Mathematics* **2022**, *10*, 615. [CrossRef]
15. Qasim, A.F.; Al-Amr, M.O. Approximate solution of the Kersten-Krasil'shchik coupled Kdv-MKdV system via reduced differential transform method. *Eurasian J. Sci. Eng.* **2018**, *4*, 1–9.

16. Kalkanli, A.K.; Sakovich, S.Y.; Yurdusen, I. Integrability of Kersten-Krasil'shchik coupled KdV-mKdV equations: Singularity analysis and Lax pair. *J. Math. Phys.* **2003**, *44*, 1703–1708. [CrossRef]
17. Hon, Y.C.; Fan, E.G. Solitary wave and doubly periodic wave solutions for the Kersten-Krasil'shchik coupled KdV-mKdV system. *Chaos Solitons Fractals* **2004**, *19*, 1141–1146. [CrossRef]
18. Goswami, A.; Singh, J.; Kumar, D. Numerical computation of fractional Kersten-Krasil'shchik coupled KdV-mKdV system occurring in multi-component plasmas. *Aims Math.* **2020**, *5*, 2346–2369.
19. Rui, W.; Qi, X. Bilinear approach to quasi-Periodic wave solutions of the Kersten-Krasil'shchik coupled KdV-mKdV system. *Bound. Value Probl.* **2016**, *2016*, 130. [CrossRef]
20. Arqub, O.A. Series solution of fuzzy differential equations under strongly generalized differentiability. *J. Adv. Res. Appl. Math.* **2013**, *5*, 31–52. [CrossRef]
21. Abu, Arqub, O.; Abo-Hammour, Z.; Al-Badarneh, R.; Momani, S. A reliable analytical method for solving higher-order initial value problems. *Discret. Dyn. Nat. Soc.* **2013**,*2013*, 673829.
22. Arqub, O.A.; El-Ajou, A.; Zhour, Z.A.; Momani, S. Multiple solutions of nonlinear boundary value problems of fractional order: A new analytic iterative technique. *Entropy* **2014**, *16*, 471–493. [CrossRef]
23. El-Ajou, A.; Arqub, O.A.; Momani, S. Approximate analytical solution of the nonlinear fractional KdV-Burgers equation: A new iterative algorithm. *J. Comput. Phys.* **2015**, *293*, 81–95. [CrossRef]
24. Xu, F.; Gao, Y.; Yang, X.; Zhang, H. Construction of fractional power series solutions to fractional Boussinesq equations using residual power series method. *Math. Probl. Eng.* **2016**, *2016*, 5492535. [CrossRef]
25. Zhang, J.; Wei, Z.; Li, L.; Zhou, C. Least-squares residual power series method for the time-fractional differential equations. *Complexity* **2019**, *2019*, 6159024. [CrossRef]
26. Yasmin, H.; Aljahdaly, N.H.; Saeed, A.M. Investigating Symmetric Soliton Solutions for the Fractional Coupled Konno-Onno System Using Improved Versions of a Novel Analytical Technique. *Mathematics* **2023**, *11*, 2686. [CrossRef]
27. Jaradat, I.; Alquran, M.; Al-Khaled, K. An analytical study of physical models with inherited temporal and spatial memory. *Eur. Phys. J. Plus* **2018**, *133*, 162. [CrossRef]
28. Mukhtar, S.; Shah, R.; Noor, S. The numerical investigation of a fractional-order multi-dimensional Model of Navier-Stokes equation via novel techniques. *Symmetry* **2022**, *14*, 1102. [CrossRef]
29. Zhang, M.F.; Liu, Y.Q.; Zhou, X.S. Efficient homotopy perturbation method for fractional non-linear equations using Sumudu transform. *Therm. Sci.* **2015**, *19*, 1167–1171. [CrossRef]
30. Ojo, G.O.; Mahmudov, N.I. Aboodh transform iterative method for spatial diffusion of a biological population with fractional-order. *Mathematics* **2021**, *9*, 155. [CrossRef]
31. Awuya, M.A.; Ojo, G.O.; Mahmudov, N.I. Solution of Space-Time Fractional Differential Equations Using Aboodh Transform Iterative Method. *J. Math.* **2022**, *2022*, 4861588. [CrossRef]
32. Awuya, M.A.; Subasi, D. Aboodh transform iterative method for solving fractional partial differential equation with Mittag-Leffler Kernel. *Symmetry* **2021**, *13*, 2055. [CrossRef]
33. Liaqat, M.I.; Etemad, S.; Rezapour, S.; Park, C. A novel analytical Aboodh residual power series method for solving linear and nonlinear time-fractional partial differential equations with variable coefficients. *AIMS Math.* **2022**, *7*, 16917–16948. [CrossRef]
34. Liaqat, M.I.; Akgul, A.; Abu-Zinadah, H. Analytical Investigation of Some Time-Fractional Black-Scholes Models by the Aboodh Residual Power Series Method. *Mathematics* **2023**, *11*, 276. [CrossRef]
35. Aboodh, K.S. The New Integral Transform'Aboodh Transform. *Glob. J. Pure Appl. Math.* **2013**, *9*, 35–43.
36. Aggarwal, S.; Chauhan, R. A comparative study of Mohand and Aboodh transforms. *Int. J. Res. Advent Technol.* **2019**, *7*, 520–529. [CrossRef]
37. Benattia, M.E.; Belghaba, K. Application of the Aboodh transform for solving fractional delay differential equations. *Univ. J. Math. Appl.* **2020**, *3*, 93–101. [CrossRef]
38. Delgado, B.B.; Macias-Diaz, J.E. On the general solutions of some non-homogeneous Div-curl systems with Riemann-Liouville and Caputo fractional derivatives. *Fractal Fract.* **2021**, *5*, 117. [CrossRef]
39. Alshammari, S.; Al-Smadi, M.; Hashim, I.; Alias, M.A. Residual Power Series Technique for Simulating Fractional Bagley-Torvik Problems Emerging in Applied Physics. *Appl. Sci.* **2019**, *9*, 5029. [CrossRef]